Contribution from the Department of Chemistry and Molecular Structure Center, Indiana University, Bloomington, Indiana 47405

Yttrium and Lanthanum Silyloxide Complexes

Michael J. McGeary, Paul S. Coan, Kirsten Folting, William E. Streib, and Kenneth G. Caulton*

Received December 20, 1990

Reaction of $[M\{N(SiMe_3)_2\}_3]$ (M = Y, La) with 3 equiv of Ph_3SiOH in toluene gave high yields of $[M(OSiPh_3)_3]_n$. The homoleptic *tris*-((triphenylsilyl)oxy)yttrium and -lanthanum complexes could be converted nearly quantitatively to monomeric Lewis base adducts, $[M(OSiPh_3)_3L_n]\cdot xL$ (M = Y, La, L = THF, n = 3, x = 1; L = pyridine, n = 3, x = 0; L = $OP(^nBu)_3$, n = 2, x = 0) by the addition of tetrahydrofuran, pyridine, or 2 equiv of $OP(^nBu)_3$, respectively. The silanol complex $[\{Y(OSiMe_2{}^tBu)_2(HOSiMe_2{}^tBu)\}\{Y(OSiMe_2{}^tBu)_2\}(\mu\text{-}OSiMe_2{}^tBu)_2]$, was isolated from the reaction of $[Y\{N(SiMe_3)_2\}_3]$ and 3.5 equiv of $HOSiMe_2{}^tBu$. This complex could be converted in high yields to $[Y(OSiMe_2{}^tBu)_3(THF)_3]$ upon exposure to excess tetrahydrofuran. Hydrogen-1 NMR studies on $[M(OSiPh_3)_3(THF)_3]\cdot THF$ (M = Y, La) and $[Y(OSiMe_2{}^tBu)_3(THF)_3]$ demonstrated that these complexes are kinetically labile on the NMR time scale with respect to exchange with free, added ligand. Low-temperature NMR studies implicated a dissociative mechanism for this process. Phosphorous-31 NMR studies in $[Y(OSiPh_3)_3\{OP(^nBu)_3\}_2]$ demonstrated that this complex participates in an exchange reaction between free and coordinated phosphine oxide via an associative mechanism. Anionic *tetrakis*((triphenylsilyl)oxy)yttrium complexes, $[K(\eta^2\text{-DME})_3(\eta^1\text{-DME})][Y(OSiPh_3)_4(\eta^2\text{-DME})]$ (**11**) and [K(18-crown-6)][$Y(OSiPh_3)_4$] (**12**), were formed by reaction of $[Y(OSiPh_3)_3]_n$ with 1 equiv of the corresponding potassium silyloxide reagent in dimethoxyethane or toluene, respectively. Single-crystal X-ray data are available for five compounds. $[Y(OSiPh_3)_3(THF)_3]\cdot THF$ (**3**) has a (i) facial arrangement of the three $-OSiPh_3$ ligands and (ii) nearly linear Y–O–Si angles [crystal data: monoclinic space group $P2_1$, a = 14.530 (7) Å, b = 16.407 (8) Å, c = 14.534 (8) Å, β = 114.32 (2)°, V = 3157.21 Å^3, Z = 2, with final residuals R = 0.0841, and R_w = 0.0790]. [$La(OSiPh_3)_3(THF)_3]\cdot THF$ (**4**) is isomorphous with **3** [crystal data: monoclinic space group $P2_1$, a = 14.830 (4) Å, b = 16.291 (4) Å, c = 14.667 (4) Å, β = 115.45 (1)°, V = 3199.32 Å^3, Z = 2, with final residuals R = 0.0464 and R_w = 0.0448]. $[Y(OSiPh_3)_3\{OP(n\text{-}Bu)_3\}_2]$ (**7**) exhibits (i) trigonal-bipyramidal coordination geometry at Y with axial $OP(^nBu)_3$ groups, and (ii) Y–O–Si angles range from 158 to 175° [Crystal data: space group $P\bar{1}$, a = 13.555 (1) Å, b = 24.035 (3) Å, c = 12.780 (1) Å, α = 100.87 (0)°, β = 114.51(0)°, γ = 86.05 (0)°, V = 3720.22 Å^3, Z = 2, with final residuals R = 0.0626 and R_w = 0.0607]. $[\{Y(OSiMe_2{}^tBu)_2(HOSiMe_2{}^tBu)\}\{Y(OSiMe_2{}^tBu)_2\}(\mu\text{-}OSiMe_2{}^tBu)_2]$ (**9**) is a (i) dinuclear complex featuring a trigonal-bipyramidal Y center linked to a tetrahedral Y center via two bridging $-OSiMe_2{}^tBu$ ligands, with (ii) an $HOSiMe_2{}^tBu$ ligand in an axial position and (iii) no hydrogen-bonding networks [crystal data: monoclinic space group $P2_1/c$, a = 17.486 (3) Å, b = 14.983 (3) Å, c = 24.286 (5) Å, β = 97.94 (1)°, V = 6301.56 Å^3, Z = 4, with Final residuals R = 0.1112 and R_w = 0.1081]. $[K(\eta^2\text{-DME})_3(\eta^1\text{-DME})][Y(OSiPh_3)_4(\eta^2\text{-DME})]$ (**11**) contains (i) a discrete K-centered cation/Y-centered anion, (ii) a seven-coordinate K cation with three chelating DME ligands and one monodentate DME ligand, and (iii) a distorted octahedral Y-centered anion [crystal data: space group $P2_1/n$, a = 14.545 (3) Å, b = 29.865 (6) Å, c = 21.726 (4) Å, β = 107.61 (1)°, V = 8995.69 Å^3, Z = 4, with final residuals R = 0.0654 and R_w = 0.0616].

Introduction

Heteropolymetallic oxide materials (e.g., $YBa_2Cu_3O_{7-x}$) have attracted considerable attention since the report of Bednorz and Müller[1] that such ceramics are capable of high-temperature electrical superconductivity. Partly because mechanisms for resistance-free conductivity are not fully understood, a flurry of activity has focused on the synthesis of new heteropolymetallic oxide materials. Traditional ceramic synthetic methods, however, require high-temperature processing, often in excess of 1000 °C, in order to achieve intimate mixing of metal sources. High-temperature processing can be undesirable for multiple reasons, including (i) increased energy cost, (ii) inability to gain access to metastable phases extant only at milder temperatures, and (iii) potential incompatibility with electronic device fabrication because of complications from diffusion between layers within the device and from stress build-up in thin films.

An alternative approach to the preparation of solid-state materials is envisioned as proceeding through molecular precursors[2] that are ligand-bridged aggregates of the sort $M_aM'_bM''_c...X_n$ (M = a metal, X = an anion). Such molecular precursors guarantee dispersion of metal sources at the **molecular** level and provide uniform reaction sites for conversion to the ceramic. Since an oxide lattice is frequently desired here, the ligand complement must be chosen, at least in part, for its ability to be subsequently removed with concomitant introduction of oxo functionality. In this regard heteropolymetallic alkoxide aggregates are relevant, since low-temperature conversion to ceramics could be available by controlled hydrolysis.[3] Alternatively, depending on the identity of the alkoxide R group, mild pyrolysis might yield the oxide lattice directly with simultaneous extrusion of ether, R_2O.

At present, heteropolymetallic alkoxide aggregates incorporating metals relevant to superconductors (i.e., heavy alkali and/or alkaline-earth metals, lanthanides, and late transition metals, especially copper) constitute a synthetic challenge; examples are only now beginning to appear.[4-6] Furthermore, even homometallic yttrium and lanthanide metal alkoxide chemistry remains poorly developed.[7-16] We now wish to report on the synthesis and characterization of homoleptic yttrium and lanthanum (triphenylsilyl)oxide aggregates, $[M(OSiPh_3)_3]_n$ (M = Y (**1**), La (**2**)), along with a series of monomeric Lewis base adducts $[M(OSiPh_3)_3L_m]\cdot xL$ (M = Y, L = THF, m = 3, x = 1 (**3**); M = La, L = THF, m = 3, x = 1 (**4**); M = Y, L = pyridine, m = 3, x = 0 (**5**); M = La, L = pyridine, m = 3, x = 0 (**6**); M = Y, L = $(^nBu)_3PO$, m = 2, x = 0, (**7**); M = La, L = $(^nBu)_3PO$, m =

(1) Bednorz, J. G.; Muller, K. A.; Takashige, M. *Science (Washington, D.C)* **1987**, *236*, 73.
(2) Hubert-Pfalzgraf, L. G. *New J. Chem.* **1987**, *11*, 663.
(3) Brinker, C. J., Clark, D. E., Ulrich, D. R., Eds. Better Ceramics Through Chemistry II. *Mater. Res. Soc. Symp. Proc.* **1986**, *73*, and references therein.
(4) Bradley, D. C.; Mehrotra, R. C.; Gaur, D. P. *Metal Alkoxides*; Academic Press: London, 1978.
(5) Caulton, K. G.; Hubert-Pfalzgraf, L. G. *Chem. Rev.* **1990**, *90*, 969.
(6) Sauer, N. N.; Garcia, E.; Salazar, K. V.; Ryan, R. D.; Martin, J. A. *J. Am. Chem. Soc.* **1990**, *112*, 1524.
(7) Mazdiyasni, K. S.; Lynch, C. T.; Smith, J. S. *Inorg. Chem.* **1966**, *5*, 342. Brown, L. M.; Mazdiyasni, K. S. *Inorg. Chem.* **1970**, *9*, 2783.
(8) Evans, W. J.; Sollberger, M. S. *J. Am. Chem. Soc.* **1986**, *108*, 6095.
(9) Evans, W. J.; Sollberger, M. S.; Hanusa, T. P. *J. Am. Chem. Soc.* **1988**, *110*, 1841.
(10) Evans, W. J.; Sollberger, M. S. *Inorg. Chem.* **1988**, *27*, 4417.
(11) Bradley, D. C.; Chudzynska, H.; Frigo, D. M.; Hursthouse, M. B.; Mazid, M. A. *J. Chem. Soc., Chem. Commun.* **1988**, 1258.
(12) Poncelet, O.; Sartain, W. J.; Hubert-Pfalzgraf, L. G.; Folting, K.; Caulton, K. G. *Inorg. Chem.* **1989**, *28*, 263.
(13) Hitchcock, P. B.; Lappert, M. F.; Singh, A. *J. Chem. Soc., Chem. Commun.* **1983**, 1499. Hitchcock, P. B.; Lappert, M. F.; Smith, R. G. *Inorg. Chim. Acta* **1987**, *139*, 183.
(14) McGeary, M. J.; Coan, P. S.; Folting, K.; Streib, W. E.; Caulton, K. G. *Inorg. Chem.* **1989**, *28*, 3283.
(15) Evans, W. J.; Olofson, J. M.; Ziller, J. W. *Inorg. Chem.* **1989**, *28*, 4308.
(16) Gradeff, P. S.; Yunlu, K.; Deming, T. J.; Olofson, J. M.; Doedens, R. J.; Evans, W. J. *Inorg. Chem.* **1990**, *29*, 420.

0020-1669/91/1330-1723$02.50/0

2, $x = 0$, (**8**)). We also articulate in this paper strategies for the elaboration of homometallic silyloxide complexes into polyheterometallic silyloxide aggregates. Accordingly, the synthesis and characterization of $[\{Y(OSiMe_2{}^tBu)_2(HOSiMe_2{}^tBu)\}\{Y(OSiMe_2{}^tBu)_2\}(\mu\text{-}OSiMe_2{}^tBu)_2]$ (**9**), $[Y(OSiMe_2{}^tBu)_3(THF)_3]$ (**10**), $[K(\eta^2\text{-DME})_3(\eta^1\text{-DME})][Y(OSiPh_3)_4(\eta^2\text{-DME})]$ (**11**), and $[K(18\text{-crown-6})][Y(OSiPh_3)_4]$ (**12**) are reported.

Experimental Section

Materials and Procedures. All manipulations were performed by using standard Schlenk techniques either in vacuo or in an atmosphere of nitrogen or by using a nitrogen-filled drybox. Solvents were dried over appropriate desiccants (potassium benzophenone ketyl for diethyl ether, pentane, hexane, dimethoxyethane, toluene, benzene, and tetrahydrofuran; P_2O_5 for dichloromethane and chloroform; and KOH for pyridine) distilled under nitrogen or in vacuo, and subjected to freeze–evacuate–thaw cycles prior to use. The compounds $[Y\{N(SiMe_3)_2\}_3]$,[17] $[La\{N(SiMe_3)_2\}_3]$,[17] and $[Li(OEt_2)N(SiMe_3)_2]_2$[18] were prepared according to literature methods. The reagents Ph_3SiOH, $Me_2(^tBu)SiOH$, [Li][^{n}Bu] (1.6 N in hexane), KH, $(^nBu)_3PO$, and 18-crown-6 ether were obtained commercially (Aldrich). Potassium hydride was purified by washing repeatedly with hexane, followed by drying in vacuo; $Me_2(^tBu)SiOH$ was vacuum distilled prior to use; $(^nBu)_3PO$ was sublimed in vacuo at ca. 80 °C; 18-crown-6 ether was similarly sublimed prior to use. Triphenylsilanol and [Li][^{n}Bu] (1.6 N in hexane) were used as received.

Physical Measurements. Infrared spectra were recorded as Nujol mulls on a Perkin-Elmer 283 spectrophotometer. Hydrogen-1 and carbon-13 NMR spectra were recorded on a Bruker AM500 (^{1}H at 500.14 MHz, ^{13}C at 125.76 MHz) instrument and referenced to $SiMe_4$. Yttrium-89 NMR spectra were recorded on a Bruker AM500 instrument at 24.5 MHz and referenced to external YCl_3 in D_2O. Phosphorous-31 and lithium-7 NMR spectra were collected on a Nicolet 360 spectrometer (^{31}P at 146.16 MHz; ^{7}Li at 140.33 MHz) and referenced to external 80% H_3PO_4 and LiBr in D_2O, respectively. NMR sample temperatures were monitored by using a thermocouple. Elemental analyses were performed either by Galbraith Laboratories, Inc., or by Oneida Research Services, Inc. Combustion aides were used in an effort to discourage carbide formation. The results of carbon, hydrogen, and nitrogen combustion analyses were sometimes variable and were not always within expectations even for crystalline samples authenticated by X-ray diffraction. In particular, experimentally determined carbon contents were often low compared with expectations, even though combustion aides (e.g., V_2O_5) were employed. In the case of $[K(\eta^2\text{-DME})_3(\eta^1\text{-DME})][Y(OSiPh_3)_4(\eta^2\text{-DME})]$, elemental analysis was further complicated by the propensity of this compound to lose dimethoxyethane coligands.

Syntheses. $[Y(OSiPh_3)_3]_n$ (**1**). A 100-mL Schlenk flask was charged with $[Y\{N(SiMe_3)_2\}_3]$ (0.18 g, 0.32 mmol) and 20 mL of toluene. The solution was cooled to 0 °C whereupon Ph_3SiOH (0.27 g, 0.98 mmol) was added in portions. A white solid precipitated after ca. 10 min. The mixture was stirred 5 h and allowed to warm gradually to room temperature. The solvent was removed in vacuo. The residue was washed repeatedly with pentane and finally dried in vacuo. Yield: 85%. IR (Nujol, cm^{-1}): no ν(OH); ν(CH) 3030; other bands 1100 (vs), 695 (s). ^{1}H NMR (CD_2Cl_2): δ 7.5–6.5 (br mult). ^{13}C{^{1}H} NMR (CD_2Cl_2): a complex set of resonances between δ 135.4 and 127.6. Anal. Calcd for $C_{54}H_{45}O_3Si_3Y$: C, 70.87; H, 4.97. Found: C, 69.99; H, 4.89.

$[La(OSiPh_3)_3]_n$ (**2**). This complex was prepared analogously to the yttrium derivative. Yield: 80%. IR (Nujol, cm^{-1}): no ν(OH); ν(CH) 3030; other bands 1100 (vs), 695 (s). ^{1}H NMR (CD_2Cl_2): δ 7.5–6.5 (br mult). ^{13}C NMR ($CDCl_3$): a complex set of resonances between δ 135.4 and 127.6. Anal. Calcd for $C_{54}H_{45}LaO_3Si_3$: C, 67.2; H, 4.69. Found: C, 68.00; H, 4.76.

$[Y(OSiPh_3)_3(THF)_3]\cdot THF$ (**3**). A 100-mL Schlenk flask was charged with $[Y(OSiPh_3)_3]_n$ (0.20 g) and 20 mL of tetrahydrofuran. A colorless solution was obtained. The mixture was stirred for ca. 4 h. The volume of the solvent was reduced in vacuo. Diethyl ether was added so as to form a layer. When this was allowed to stand in the freezer (−20 °C), nicely formed crystals, suitable for X-ray diffraction, precipitated. Yield: 95%. IR (Nujol, cm^{-1}): no ν(OH); ν(CH) 3040, 3020; aromatic overtones 1945, 1875, 1810, 1760; other bands 1100 (vs); 695 (s). ^{1}H NMR (THF-d_8): δ 7.65 (d, 6.7 Hz, 18 H, ortho H), 7.09 (t, 7.5 Hz, 9 H, para H), 6.94 (~t, 7.1 Hz, 18 H, meta H), 3.58 (m, 16 H, THF), 1.74 (m, 16 H, THF). ^{13}C NMR (THF-d_8): δ 142.4 (ipso), 136.4 (ortho), 128.7 (para), 127.8 (meta), 68.2 (THF), 26.4 (THF). Anal. Calcd for $C_{70}H_{77}O_7Si_3Y$: C, 69.85; H, 6.46. Found: C, 66.88; H, 6.15.

$[La(OSiPh_3)_3(THF)_3]\cdot THF$ (**4**). The lanthanum complex was prepared analogously to **3**. Crystals suitable for diffraction were obtained by similar procedures. Yield: 95%. IR (Nujol, cm^{-1}): no ν(OH); ν(CH) 3040, 3020; aromatic overtones 1950, 1870, 1760; other bands 1100 (vs); 695 (s). ^{1}H NMR ($CDCl_3$): δ 7.49 (d, 6.3 Hz, 18 H, ortho), 7.11 (t, 7.4 Hz, 9 H, para), 7.00 (dd, 6.3, 7.4 Hz, 18 H, meta), 3.49 (br, 16 H, THF), 1.43 (t, 1.3 Hz, 16 H, THF). ^{13}C NMR ($CDCl_3$): δ 141.1 (ipso), 135.0 (ortho), 128.31 (para), 127.2 (meta), 68.9 (THF), 25.2 (THF). Anal. Calcd for $C_{70}H_{77}LaO_7Si_3$: C, 67.06, H, 6.20. Found: C, 66.99; H, 6.19.

$[Y(OSiPh_3)_3(py)_3]$ (**5**). A small amount of $[Y(OSiPh_3)_3]_n$ was loaded into a 100-mL Schlenk flask. Pyridine (10 mL) was condensed onto the solid at −196 °C. When this was thawed, a colorless solution was obtained. Stirring was maintained for 12 h, whereupon the sample was concentrated in vacuo. Diethyl ether was added so as to form a layer. Colorless crystals precipitated at −20 °C after 24 h. These were decanted, washed with ether, and finally dried in vacuo. IR (Nujol, cm^{-1}) ν(CH) 3040, 3020; ν(CN) 1590; other bands 1100 (vs), 695 (s). ^{1}H NMR ($CDCl_3$): δ 8.35 (br, s, 6 H, 2,6-py), 7.42 (br m, 3 H, 4-py), 7.37 (d, 7.0 Hz, 18 H, ortho H), 7.10 (t, 7.4 Hz, 9 H, para H), 6.93 (~t, 7.4 Hz, 18 H, meta H), 6.74 (br s, 6 H, 3,5-py). ^{13}C NMR ($CDCl_3$): δ 149.9 (2,6-py), 140.8 (ipso), 137.6 (4-py), 135.2 (ortho), 128.1 (meta), 127.1 (para), 123.8 (3,5-py). Anal. Calcd for $C_{69}H_{60}N_3O_3Si_3Y$: C, 71.90; H, 5.26, N, 3.65. Found: C, 71.08; H, 5.60; N, 3.44.

$[La(OSiPh_3)_3(py)_3]$ (**6**). The lanthanum complex, **6**, was prepared analogously to **5** and isolated as a colorless crystalline solid. IR (Nujol, cm^{-1}): ν(CH) 3030; ν(CN) 1582; other bands 1100, 695. ^{1}H NMR ($CDCl_3$): δ 8.42 (d, 7.4 Hz, 6 H, 2,6-py), 7.54 (t, 7.7 Hz, 3 H, 4-py), 7.45 (d, 7.15 Hz, 18 H, ortho), 7.19 (t, 7.7 Hz, 9 H, para), 7.02 (t, 7.5 Hz, 18 H, meta), 6.92 (t, 7.5 Hz, 6 H, 3,5-py). ^{13}C NMR ($CDCl_3$): δ 149.5 (2,6-py), 141.2 (ipso), 137.0 (4-py), 135.1 (ortho), 128.1 (para), 127.1 (meta), 123.9 (3,5-py). Anal. Calcd for $C_{69}H_{60}N_3O_3Si_3La$: C, 68.91; H, 5.04; N, 3.50. Found: C, 69.13; H, 5.01; N, 4.17.

$[Y(OSiPh_3)_3\{OP(^nBu)_3\}_2]$ (**7**). A 100-mL Schlenk flask was charged with 0.46 g of $[Y(OSiPh_3)]_n$ and 0.22 g (1.00 mmol) of $OP(^nBu)_3$. Hexane (30 mL) was added, and the resultant solution was stirred for 3 h. The sample was concentrated in vacuo to 10 mL. Large colorless crystals suitable for X-ray diffraction precipitated overnight at 0 °C. These were decanted, washed with cold pentane, and dried in vacuo. Yield: 80%. IR (Nujol, cm^{-1}): ν(CH) 3110, 3040, 3010; aromatic overtones 1940, 1875, 1810, 1755; ν(P=O) 1145 cm^{-1}. ^{1}H NMR ($CDCl_3$): δ 7.72 (d, 6.6 Hz, 18 H, ortho), 7.25 (t, 6.9 Hz, 9 H, para), 7.21 (~t, 6.7 Hz, 18 H, meta), 1.03 (br, 12 H, P–CH_2–), 0.86 (m, 12 H, P–C–CH_2–), 0.80 (m, 12 H, P–C–C–CH_2–), 0.45 (~t, 18 H, CH_3). ^{13}C NMR ($CDCl_3$): δ 141.7 (ipso), 135.3 (ortho), 128.1 (para), 127.1 (meta), 25.6 (d, $^1J_{PC}$ = 66.1 Hz, P–CH_2–), 23.6 (d, $^2J_{PC}$ = 14.2 Hz, P–C–CH_2–), 23.2 (P–C–C–CH_2–), 13.2 (CH_3). ^{31}P NMR ($CDCl_3$): δ 58.2 (d, $^2J_{YP}$ = 7.3 Hz). Anal. Calcd for $C_{78}H_{99}O_5P_2Si_3Y$: C, 69.29; H, 7.40. Found: C, 69.52; H, 7.75.

$[La(OSiPh_3)_3\{OP(^nBu)_3\}_2]$ (**8**). The lanthanum complex was prepared analogously to **7**. Yield: 80%. IR (Nujol, cm^{-1}): ν(CH) 3040, 3020; aromatic overtones 1940, 1870, 1810, 1750; ν(PO) 1100; other bands 695. ^{1}H NMR ($CDCl_3$): δ 7.65, 7.24, 7.20 (br, m, 45 H, phenyl region), 1.15, (br, 12 H, P–CH_2–), 1.00 (br, 12 H, P–C–CH_2–), 0.88 (br, 12 H, P–C–C–CH_2–), 0.54 (br, 18 H, CH_3). ^{13}C NMR ($CDCl_3$): δ 141.4 (ipso), 135.2 (ortho), 128.2 (para), 127.2 (meta), 26.6 (d, $^1J_{PC}$ = 60.0 Hz, P–C–), 23.8 (br, P–C–CH_2–), 23.4 (P–C–C–CH_2–), 13.3 (CH_3). ^{31}P NMR ($CDCl_3$): δ 57.6. Anal. Calcd for $C_{78}H_{99}LaO_5P_2Si_3$: C, 66.82; H, 7.13. Found: C, 66.92; H, 6.96.

$[\{Y(OSiMe_2{}^tBu)_2(HOSiMe_2{}^tBu)\}\{Y(OSiMe_2{}^tBu)_2\}(\mu\text{-}OSiMe_2{}^tBu)_2]$ (**9**). A 100-mL Schlenk flask was charged with 1.00 g (1.75 mmol) of $[Y\{N(SiMe_3)_2\}_3]$ and 50 mL of hexane. The solution was cooled to 0 °C whereupon 0.96 mL (6.12 mmol) of $HOSiMe_2{}^tBu$ was added via pipette. The mixture was allowed to gradually warm to room temperature while stirring was maintained. After 3 h, the sample was concentrated in vacuo. Large colorless crystals suitable for X-ray diffraction precipitated during storage at −20 °C for 24 h. These were decanted and dried in vacuo. Yield: 60%. IR (Nujol, cm^{-1}): ν(OH) 3320 (br); other bands 1249, 985, 960, 930, 920, 910, 840, 780, 760, 650 cm^{-1}. ^{1}H NMR ($CDCl_3$): δ 1.64 (s, 1 H, OH), 0.88 (s, 63 H, ^{t}Bu), 0.04 (s, 42 H, SiMe). ^{13}C NMR ($CDCl_3$): δ 26.1 (^{t}Bu), 18.2 (–CMe_3), −2.4 (SiMe). Anal. Calcd for $C_{42}H_{106}O_7Si_7Y_2$: C, 45.94; H, 9.75. Found: C, 45.86; H, 9.90.

$[Y(OSiMe_2{}^tBu)_3(THF)_3]$ (**10**). A 100-mL Schlenk flask was charged with a small amount of $[\{Y(OSiMe_2{}^tBu)_2(HOSiMe_2{}^tBu)\}\{Y(OSiMe_2{}^tBu)_2\}(\mu\text{-}OSiMe_2{}^tBu)_2]$. Tetrahydrofuran (10 mL) was added. The solution was stirred for 12 h. The solvent was removed in vacuo to give an oily paste. The paste was extracted into a minimum of pentane. Cooling to −20 °C for 24 h caused large colorless crystals to precipitate. IR (Nujol, cm^{-1}): 1235, 1030, 960, 875, 820, 755, 650. ^{1}H NMR ($CDCl_3$): δ 3.87 (m, 12 H, THF), 1.88 (m, 12 H, THF), 0.85 (s, 27 H,

(17) Bradley, D. C.; Ghotra, J. S.; Hart, F. A. *J. Chem. Commun., Dalton Trans.* **1973**, 1021.
(18) Harris, D. H.; Lappert, M. F. *J. Organomet. Chem.* **1976**, *2*, 13.

Table I. Crystal Data for $[M(OSiPh_3)_3(THF)_3]\cdot THF$

	M = Y	M = La
chemical formula	$C_{70}H_{77}O_7Si_3Y$	$C_{70}H_{77}O_7Si_3La$
a, Å	14.530 (7)	14.830 (4)
b, Å	16.407 (8)	16.291 (4)
c, Å	14.534 (8)	14.667 (4)
β, deg	114.32 (2)	115.45 (1)
V, Å^3	3157.21	3199.32
Z	2	2
fw	1203.54	1253.54
space group	$P2_1$	$4P2_1$
T, °C	−157	−144
λ, Å	0.71069	0.71069
ρ_{calcd}, g cm^{-3}	1.266	1.301
μ(Mo Kα), cm^{-1}	10.3	7.74
R	0.0841	0.0464
R_w	0.0790	0.0448

^{t}Bu), −0.06 (s, 18 H, SiMe). ^{13}C NMR ($CDCl_3$): δ 68.9 (THF), 26.6 (^{t}Bu), 25.5 (THF), 18.7 (−CMe_3), −1.5 (SiMe). Anal. Calcd for $C_{30}H_{69}O_6Si_3Y$: C, 51.53; H, 9.97. Found: C, 51.11; H, 9.93.

$[K(\eta^2\text{-DME})_3(\eta^1\text{-DME})][Y(OSiPh_3)_4(\eta^2\text{-DME})]$ (11). A 100-mL Schlenk flask was charged with 0.54 g (0.60 mmol) of $[Y(OSiPh_3)_3]_n$ and 0.20 g (0.60 mmol) of $[K(THF)_{0.2}(OSiPh_3)]$.[19] Tetrahydrofuran (20 mL) was added, and the mixture was stirred for 12 h. The solvent was evaporated in vacuo. The residue was extracted into warm DME, and the resultant suspension was filtered to remove trace particulates. The volume of the solution was reduced in vacuo. Hexane was added to form a layer. Colorless crystals suitable for X-ray diffraction precipitated when this mixture was allowed to stand for 12 h at 0 °C. These were decanted, washed with pentane, and dried in vacuo. Yield: 80%. IR (Nujol, cm^{-1}): ν(CH) 3100, 3020; aromatic overtones 1950, 1880, 1815, 1760; other bands 1095, 965, 850, 735, 695. ^{1}H NMR ($CDCl_3$, 298 K): δ 7.64 (d, 7.2 Hz, 24 H, ortho), 7.19 (t, 7.4 Hz, 12 H, para), 7.00 (t, 7.4 Hz, 24 H, meta), 3.19 (vbr s, DME). Note: The integrated intensity ratio of the phenyl region to the DME region varied from sample to sample. ^{13}C NMR ($CDCl_3$, 298 K): δ 141.1 (ipso), 135.5 (ortho), 128.5 (para), 127.5 (meta), 71.4 (OCH_2), 59.8 (OCH_3). Anal. Calcd for $C_{92}H_{110}KO_{14}Si_4Y$: C, 65.75; H, 6.61. Found: C, 67.75; H, 5.53.

$[K(18\text{-crown-}6)][Y(OSiPh_3)_4]$ (12). A 100-mL Schlenk flask was charged with 0.27 g (0.30 mmol) of $[Y(OSiPh_3)_3]_n$ and 20 mL of toluene. The reagent, $[K(18\text{-crown-}6)(OSiPh_3)]$[19] (0.18 g, 0.30 mmol), was added as a solid in portions. The mixture was stirred for 24 h. An oily solid precipitated after ca. 2 h. The volume of solvent was reduced in vacuo. The precipitate was decanted, triturated to a powder with diethyl ether followed by pentane, and finally dried in vacuo. Yield: 75%. IR (Nujol, cm^{-1}): ν(CH) 3080, 3050; aromatic overtones 1965, 1890, 1830, 1790; other bands 1107, 981, 705. ^{1}H NMR (C_6D_6): δ 7.99 (d, 6.5 Hz, 24 H, ortho), 7.14 (~t, 7.3 Hz, 12 H, para), 7.08 (~t, 7.2 Hz, 24 H, meta), 2.81 (s, 24 H, OCH_2). ^{13}C NMR (C_6D_6): δ 142.4 (ipso), 135.8 (ortho), 127.6 (meta), para carbon obscured by C_6D_6, 69.9 (OCH_2). Anal. Calcd for $C_{84}H_{84}KO_{10}Si_4Y$: C, 67.52; H, 5.68. Found: C, 65.16; H, 5.56.

Lack of Reaction Between $[Y(OSiPh_3)_3]_n$ and $[Li(OSiPh_3)]_x$. A 100-mL Schlenk flask was charged with 0.20 g (0.22 mol) of $[Y(OSiPh_3)_3]_n$ and 0.07 g (0.22 mmol) of $[Li(OSiPh_3)]_x$.[19] Tetrahydrofuran (20 mL) was added and the resultant solution was stirred for 20 h. The sample was concentrated in vacuo and diethyl ether was added so as to form a layer. Crystals precipitated after standing 12 h at −20 °C. These were isolated by decantation, washed with ether, and dried in vacuo. Yield: 70%. The crystalline product was identified as $[Y(OSiPh_3)_3(THF)_3]\cdot THF$ by comparison of IR and ^{1}H and ^{13}C NMR data. The absence of lithium in the product was confirmed by a negative flame test and the lack of a lithium-7 NMR signal.

X-ray Diffraction Study of $[Y(OSiPh_3)_3(THF)_3]\cdot THF$. A suitable small crystal was transferred under N_2 to a goniostat where it was cooled to −157 °C for characterization and data collection. A systematic automated search of a limited hemisphere of reciprocal space yielded a set of reflections that exhibited monoclinic symmetry ($2/m$). The systematic extinction of $0k0$ for $k = 2n + 1$ led to the possible space groups $P2_1$ or $P2_1/m$. Choice of the noncentrosymmetric space group $P2_1$ was confirmed by the successful solution and refinement of the structure. Unit cell dimensions (Table I) were determined by least-squares fit of 41 unique reflections centered at plus and minus 2θ. Data collection[20] ($6° \le 2\theta \le 45°$) was undertaken as detailed in Table I. A plot of the standard reflections measured periodically during the data collection showed no significant trends. No absorption correction was performed.

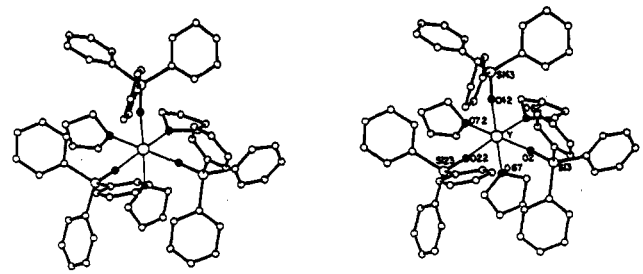

Figure 1. Stereo ORTEP drawing of the $M(THF)_3(OSiPh_3)_3$ unit (M = Y or La), showing selected atom labeling. The view is down an approximate C_3 axis of the yttrium compound. Oxygens are stippled.

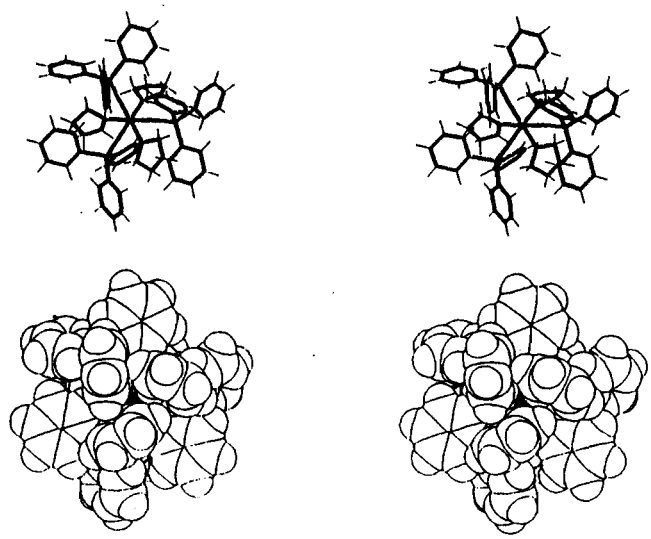

Figure 2. Stereo stick figure and space-filling drawings of $[Y(OSiPh_3)_3(THF)_3]$, viewed as in Figure 1.

The structure was solved by locating the Y atom by means of direct methods (MULTAN). The remaining atoms were located in successive difference Fourier maps phased with the already known atoms. The asymmetric unit contains an interstitial molecule of THF (O(77)–C(81)) in addition to the Y complex. Due to the large number of structural parameters (331 for isotropic refinement of all non-hydrogen atoms and anisotropic Y) as well as the relatively weak data (giving a ratio of obs/param = 5.8), no attempts were made at refining all atoms anisotropically. Hydrogen atoms were included in fixed, idealized (d_{CH} = 0.95 Å) positions. The final difference map was essentially featureless; the largest peak was 0.56 e/Å^3 in the vicinity of the Y atom. The results of the structural study are shown in Tables II and III and Figures 1 and 2. All figures employ 50% probability ellipsoids.

Crystallography of $[La(OSiPh_3)_3(THF)_3]\cdot THF$. A suitable, well-formed crystal was transferred to the goniostat, where it was cooled to −144 °C for characterization and data collection. A systematic search of a limited hemisphere of reciprocal space yielded a set of reflections that exhibited monoclinic symmetry. The systematic extinction of $0k0$ for $k = 2n + 1$ limited the choice of possible space groups to $P2_1$, or $P2_1/m$. The choice of the noncentrosymmetric space group $P2_1$ was confirmed by the successful solution and refinement of the structure. This crystal is isomorphous with that of the yttrium analogue. Data collection[20] ($6° \le 2\theta \le 45°$), Table I, and reduction yielded a unique set of 3901 reflections for a criterion of $F > 3.0\sigma(F)$. This data set was of better quality than for the yttrium analogue. The R for the averaging was 0.034 for 1263 reflections measured more than once. A plot of the standard reflections showed no significant decay. No correction for absorption was performed.

Refinement was initiated by using the parameters of the isomorphous yttrium compound. The least-squares refinement was completed by using anisotropic thermal parameters on all non-hydrogen atoms and introducing hydrogen atoms in fixed, calculated positions.

To determine the absolute configuration of the crystal selected, the reflections were reprocessed in such a way that Friedel pairs were *not* averaged. The resulting 4801 unique reflections gave R = 0.0498 and R_w = 0.047 for the structure shown in this report while, for the enantiomer, the corresponding values were 0.052 and 0.050. The final dif-

(19) McGeary, M. J.; Caulton, K. G. Manuscript in preparation.
(20) Huffman, J. C.; Lewis, L. N.; Caulton, K. G. *Inorg. Chem.* **1980**, *19*, 1840.

Table II. Fractional Coordinates[a,b] and Isotropic Thermal Parameters[c] for $[Y(OSiPh_3)_3(THF)_3]\cdot THF$

	x	y	z	$10B_{iso}$, Å^2		x	y	z	$10B_{iso}$, Å^2
Y(1)	1838 (2)	4927*	7931 (2)	16	O(42)	2683 (13)	5817 (12)	7527 (13)	24 (4)
O(2)	2135 (13)	5300 (11)	9434 (12)	27 (4)	Si(43)	3352 (6)	6481 (5)	7345 (6)	21 (2)
Si(3)	2230 (6)	5660 (5)	10485 (6)	20 (2)	C(44)	2785 (21)	7526 (17)	7334 (20)	22 (6)
C(4)	1032 (21)	5431 (18)	10678 (21)	27 (6)	C(45)	1816 (22)	7580 (18)	7258 (21)	27 (6)
C(5)	147 (19)	5206 (15)	9826 (18)	20 (6)	C(46)	1305 (27)	8325 (23)	7167 (26)	41 (8)
C(6)	−747 (21)	5027 (26)	9947 (21)	39 (7)	C(47)	1891 (27)	9011 (22)	7288 (26)	44 (8)
C(7)	−764 (23)	5103 (24)	10863 (23)	47 (8)	C(48)	2859 (26)	8989 (22)	7317 (25)	42 (8)
C(8)	88 (23)	5277 (19)	11712 (23)	40 (7)	C(49)	3303 (24)	8239 (20)	7366 (22)	36 (7)
C(9)	1016 (22)	5487 (19)	11630 (22)	32 (7)	C(50)	4704 (20)	6447 (17)	8341 (19)	18 (6)
C(10)	3320 (19)	5190 (15)	11571 (18)	19 (6)	C(51)	4936 (26)	6070 (22)	9260 (25)	44 (8)
C(11)	4252 (22)	5522 (18)	12042 (21)	29 (6)	C(52)	5970 (35)	6005 (29)	9998 (33)	76 (10)
C(12)	5023 (23)	5151 (21)	12833 (23)	40 (7)	C(53)	6680 (33)	6226 (28)	9732 (34)	72 (10)
C(13)	4900 (27)	4410 (22)	13165 (25)	39 (8)	C(54)	6542 (29)	6647 (24)	8853 (29)	55 (9)
C(14)	4019 (26)	4013 (21)	12690 (25)	42 (8)	C(55)	5496 (22)	6709 (18)	8128 (21)	26 (6)
C(15)	3177 (26)	4395 (20)	11888 (24)	39 (7)	C(56)	3373 (24)	6315 (21)	6069 (24)	38 (7)
C(16)	2485 (18)	6786 (16)	10587 (18)	15 (5)	C(57)	2788 (25)	6802 (21)	5195 (25)	44 (8)
C(17)	2645 (26)	7197 (22)	9835 (26)	44 (8)	C(58)	2731 (26)	6636 (23)	4241 (26)	47 (8)
C(18)	2843 (24)	8037 (21)	9871 (23)	37 (7)	C(59)	3304 (23)	5948 (20)	4151 (22)	32 (7)
C(19)	2828 (26)	8481 (22)	10629 (26)	44 (8)	C(60)	3887 (25)	5506 (21)	4949 (25)	43 (8)
C(20)	2698 (26)	8060 (22)	11431 (25)	44 (8)	C(61)	3923 (22)	5674 (20)	5890 (22)	35 (7)
C(21)	2531 (23)	7238 (20)	11387 (22)	34 (7)	O(62)	3303 (16)	4065 (13)	8652 (15)	36 (5)
O(22)	337 (14)	5334 (12)	7109 (14)	32 (4)	C(63)	4002 (26)	4022 (22)	9701 (26)	45 (8)
Si(23)	−696 (7)	5818 (6)	6535 (7)	28 (2)	C(64)	4627 (32)	3295 (29)	9888 (34)	78 (11)
C(24)	−739 (19)	6820 (16)	7208 (18)	13 (5)	C(65)	4409 (35)	2975 (30)	8837 (36)	84 (11)
C(25)	−1465 (23)	7392 (19)	6800 (22)	32 (7)	C(66)	3858 (39)	3631 (33)	8177 (37)	88 (12)
C(26)	−1469 (25)	8049 (22)	7380 (25)	47 (8)	O(67)	1072 (16)	3687 (13)	8265 (15)	36 (5)
C(27)	−727 (22)	8193 (19)	8325 (22)	30 (7)	C(68)	10 (32)	3519 (27)	7820 (30)	61 (10)
C(28)	23 (21)	7633 (18)	8722 (20)	21 (6)	C(69)	−131 (43)	2972 (36)	8505 (41)	102 (13)
C(29)	22 (23)	6974 (19)	8202 (22)	24 (6)	C(70)	804 (33)	2607 (27)	9163 (30)	63 (9)
C(30)	−1815 (20)	5237 (16)	6432 (19)	22 (6)	C(71)	1603 (29)	3171 (25)	9142 (28)	60 (9)
C(31)	−2152 (26)	4502 (21)	5775 (25)	40 (7)	O(72)	1675 (15)	4182 (12)	6471 (14)	30 (4)
C(32)	−2997 (29)	4116 (24)	5754 (28)	54 (9)	C(73)	1847 (31)	4505 (25)	5654 (32)	64 (10)
C(33)	−3510 (30)	4326 (25)	6316 (30)	59 (9)	C(74)	956 (37)	4187 (31)	4700 (36)	83 (11)
C(34)	−3253 (22)	5050 (26)	6911 (21)	43 (7)	C(75)	668 (48)	3399 (43)	5106 (51)	137 (15)
C(35)	−2390 (25)	5435 (20)	6977 (23)	39 (7)	C(76)	1205 (47)	3431 (42)	6099 (49)	128 (15)
C(36)	−891 (23)	6054 (19)	5175 (22)	30 (7)	O(77)	4129 (24)	3193 (22)	14950 (24)	100 (9)
C(37)	−1863 (22)	6060 (18)	4367 (22)	29 (6)	C(78)	4259 (21)	3185 (18)	15979 (21)	23 (6)
C(38)	−1948 (21)	6222 (18)	3353 (21)	25 (6)	C(79)	4478 (27)	2338 (24)	16306 (27)	54 (9)
C(39)	−1128 (26)	6381 (21)	3152 (25)	39 (8)	C(80)	4198 (25)	1831 (22)	15416 (25)	46 (8)
C(40)	−180 (26)	6410 (22)	3997 (26)	46 (8)	C(81)	4372 (24)	2392 (21)	14656 (24)	39 (7)
C(41)	−45 (23)	6251 (19)	5008 (22)	29 (6)					

[a] Fractional coordinates are × 10^4. [b] Parameters marked by an asterisk were not varied. [c] Isotropic values for those atoms refined anisotropically are calculated by using the formula given by Hamilton: Hamilton, W. C. *Acta Crystallogr.* **1959**, *12*, 609.

Table III. Selected Bond Distances (Å) and Angles (deg) for $[M(OSiPh_3)_3(THF)_3]\cdot THF$

	M = Y	M = La		M = Y	M = La		M = Y	M = La
M(1)–O(2)	2.136 (17)	2.228 (6)	Si(3)–O(2)	1.589 (18)	1.596 (7)	Si(23)–C(30)	1.838 (27)	1.864 (10)
M(1)–O(22)	2.118 (18)	2.246 (7)	Si(3)–C(4)	1.91 (3)	1.899 (11)	Si(23)–C(36)	1.92 (3)	1.891 (10)
M(1)–O(42)	2.138 (18)	2.203 (7)	Si(3)–C(10)	1.880 (26)	1.878 (9)	Si(43)–O(42)	1.554 (19)	1.596 (7)
M(1)–O(62)	2.406 (21)	2.635 (8)	Si(3)–C(16)	1.878 (27)	1.877 (11)	Si(43)–C(44)	1.90 (3)	1.883 (10)
M(1)–O(67)	2.462 (21)	2.650 (8)	Si(23)–O(22)	1.597 (20)	1.600 (7)	Si(43)–C(50)	1.901 (27)	1.886 (12)
M(1)–O(72)	2.374 (20)	2.644 (7)	Si(23)–C(24)	1.927 (26)	1.873 (10)	Si(43–C(56)	1.89 (3)	1.893 (10)
O(2)–M(1)–O(22)	102.3 (7)	101.89 (26)	O(62)–M(1)–O(72)	80.3 (7)	78.63 (23)	M(1)–O(22)–Si(23)	168.5 (12)	167.9 (4)
O(2)–M(1)–O(42)	100.8 (7)	101.68 (27)	O(67)–M(1)–O(72)	82.2 (7)	82.29 (25)	M(1)–O(42)–Si(43)	174.4 (11)	173.1 (5)
O(2)–M(1)–O(62)	87.3 (7)	89.11 (26)	O(2)–Si(3)–C(4)	110.2 (12)	109.3 (4)	M(1)–O(62)–C(63)	126.9 (19)	125.6 (9)
O(2)–M(1)–O(67)	87.3 (7)	86.75 (26)	O(2)–Si(3)–C(10)	111.4 (11)	112.1 (4)	M(1)–O(62)–C(66)	130.4 (24)	128.1 (8)
O(2)–M(1)–O(72)	165.0 (7)	165.31 (23)	O(2)–Si(3)–C(16)	112.1 (11)	112.2 (4)	C(63)–O(62)–C(66)	101 (3)	104.4 (12)
O(22)–M(1)–O(42)	101.8 (7)	104.98 (26)	O(22)–Si(23)–C(24)	112.3 (11)	111.1 (4)	M(1)–O(67)–C(68)	124.1 (22)	123.8 (7)
O(22)–M(1)–O(62)	162.1 (7)	157.67 (26)	O(22)–Si(23)–C(30)	113.2 (12)	111.8 (4)	M(1)–O(67)–C(71)	122.2 (20)	121.4 (8)
O(22)–M(1)–O(67)	85.8 (7)	86.37 (26)	O(22)–Si(23)–C(36)	110.4 (12)	109.5 (4)	C(68)–O(67)–C(71)	111.5 (27)	109.3 (11)
O(22)–M(1)–O(72)	87.6 (7)	87.18 (23)	O(42)–Si(43)–C(44)	109.5 (11)	110.5 (4)	M(1)–O(72)–C(73)	124.8 (21)	120.8 (7)
O(42)–M(1)–O(62)	90.9 (7)	91.5 (3)	O(42)–Si(43)–C(50)	111.9 (11)	110.6 (5)	M(1)–O(72)–C(76)	131 (3)	130.2 (9)
O(42)–M(1)–O(67)	167.3 (7)	163.9 (3)	O(42)–Si(43)–C(56)	109.3 (13)	110.1 (4)	C(73)–O(72)–C(76)	103 (3)	102.0 (10)
O(42)–M(1)–O(72)	87.9 (7)	86.83 (25)	M(1)–O(2)–Si(3)	172.2 (11)	177.0 (5)	C(78)–O(77)–C(81)	111 (3)	109.8 (10)
O(62)–M(1)–O(67)	79.6 (7)	74.8 (3)						

ference Fourier was essentially featureless; the largest peak was 0.85 e/Å^3. The results of the structure determination are shown in Tables III and IV and Figure 1.

Structure Determination of $[Y(OSiPh_3)_3\{OP(^nBu)_3\}_2]$. A suitable crystal was transferred to the goniostat where it was cooled to −156 °C for characterization and data collection. A systematic manual search of a limited hemisphere of reciprocal space yielded a set of reflections that exhibited no symmetry (other than $\bar{1}$) and no systematic extinctions. The choice of the centrosymmetric space group $P\bar{1}$ was confirmed by the subsequent solution and refinement of the structure. Unit cell dimensions (Table V) were determined by using 60 reflections having $19° < 2\theta < 37°$. Data collection yielded a unique set of 9747 reflections.[20] The R for the averaging was 0.025 for 1254 reflections measured more than once. Plots of the standard reflections monitored periodically during the data collection showed no significant variations. Following an inspection of the intensity data, no correction for absorption was performed.

The structure was solved by the usual combination of direct methods and Fourier techniques. The initial E map from MULTAN revealed the

Table IV. Fractional Coordinates[a,b] and Isotropic Thermal Parameters[c] for $[La(OSiPh_3)_3(THF)_3]\cdot THF$

atom	x	y	z	$10B_{iso}$, Å^2	atom	x	y	z	$10B_{iso}$, Å^2
La(1)	1849.9 (4)	4927*	7893.8 (3)	27	O(42)	2848 (5)	5776 (5)	7595 (5)	42
O(2)	2056 (6)	5330 (5)	9423 (5)	42	Si(43)	3466 (2)	6471 (2)	7343 (2)	30
Si(3)	2181 (2)	5664 (2)	10494 (2)	34	C(44)	2926 (7)	7514 (6)	7354 (6)	27
C(4)	984 (8)	5468 (6)	10635 (7)	33	C(45)	1971 (8)	7558 (7)	7297 (7)	34
C(5)	116 (8)	5250 (6)	9807 (7)	35	C(46)	1537 (8)	8308 (8)	7310 (8)	41
C(6)	−761 (7)	5061 (7)	9911 (8)	47	C(47)	2047 (9)	9016 (7)	7325 (9)	44
C(7)	−772 (8)	5103 (7)	10850 (8)	46	C(48)	2958 (9)	8992 (7)	7364 (9)	45
C(8)	70 (9)	5327 (7)	11676 (9)	42	C(49)	3426 (8)	8247 (6)	7402 (8)	34
C(9)	925 (9)	5513 (7)	11572 (8)	44	C(50)	4829 (9)	6420 (7)	8256 (9)	48
C(10)	3203 (7)	5117 (5)	11571 (7)	31	C(51)	5087 (12)	5975 (9)	9165 (11)	78
C(11)	4152 (8)	5432 (7)	12075 (8)	42	C(52)	6210 (17)	5931 (10)	9841 (13)	99
C(12)	4885 (8)	4970 (15)	12858 (10)	77	C(53)	6827 (14)	6312 (12)	9526 (14)	89
C(13)	4691 (12)	4233 (12)	13151 (10)	75	C(54)	6593 (11)	6740 (11)	8673 (13)	78
C(14)	3759 (12)	3940 (9)	12661 (10)	64	C(55)	5580 (9)	6775 (10)	8056 (11)	66
C(15)	3031 (9)	4340 (8)	11865 (8)	45	C(56)	3424 (7)	6285 (6)	6051 (7)	30
C(16)	2509 (8)	6784 (7)	10667 (8)	40	C(57)	2818 (8)	6721 (7)	5221 (8)	37
C(17)	2641 (10)	7202 (8)	9897 (8)	56	C(58)	2740 (9)	6524 (9)	4256 (8)	49
C(18)	2877 (12)	8013 (10)	9968 (11)	72	C(59)	3273 (9)	5886 (10)	4149 (9)	58
C(19)	2939 (11)	8464 (8)	10809 (11)	57	C(60)	3866 (9)	5420 (9)	4967 (9)	56
C(20)	2833 (12)	8065 (9)	11585 (12)	68	C(61)	3936 (7)	5636 (7)	5889 (8)	39
C(21)	2622 (10)	7226 (7)	11492 (9)	51	O(62)	3308 (7)	3860 (5)	8752 (6)	64
O(22)	300 (5)	5378 (4)	6917 (5)	36	C(63)	4061 (13)	3890 (9)	9788 (10)	84
Si(23)	−724 (2)	5873 (2)	6355 (2)	30	C(64)	4709 (16)	3294 (19)	9924 (12)	153
C(24)	−712 (8)	6842 (6)	7048 (8)	34	C(65)	4483 (13)	2869 (13)	8964 (14)	98
C(25)	−1425 (8)	7447 (7)	6634 (9)	44	C(66)	3695 (17)	3276 (14)	8267 (13)	131
C(26)	−1415 (11)	8150 (7)	7213 (12)	59	O(67)	983 (7)	3595 (5)	8188 (6)	59
C(27)	−703 (10)	8214 (8)	8164 (11)	57	C(68)	−78 (11)	3462 (8)	7726 (12)	66
C(28)	9 (10)	7637 (8)	8596 (10)	52	C(69)	−239 (19)	2959 (13)	8473 (26)	141
C(29)	−6 (10)	6950 (7)	8025 (8)	45	C(70)	628 (22)	2651 (13)	9199 (16)	121
C(30)	−1822 (7)	5254 (6)	6249 (8)	32	C(71)	1434 (15)	3130 (9)	9133 (11)	91
C(31)	−2147 (9)	4558 (7)	5634 (9)	46	O(72)	1742 (6)	4082 (4)	6312 (5)	41
C(32)	−2949 (10)	4108 (7)	5535 (10)	57	C(73)	1611 (11)	4533 (9)	5308 (13)	79
C(33)	−3466 (10)	4329 (9)	6089 (10)	65	C(74)	600 (9)	4246 (8)	4605 (9)	51
C(34)	−3187 (8)	5005 (10)	6721 (8)	54	C(75)	423 (13)	3602 (15)	5156 (14)	104
C(35)	−2363 (9)	5451 (7)	6807 (8)	45	C(76)	1322 (14)	3326 (11)	5955 (14)	88
C(36)	−918 (7)	6135 (6)	5028 (7)	32	O(77)	4297 (9)	3145 (7)	15050 (8)	90
C(37)	−1856 (7)	6097 (7)	4206 (8)	39	C(78)	4277 (10)	3107 (8)	15961 (11)	57
C(38)	−1964 (9)	6273 (8)	3217 (8)	47	C(79)	4384 (13)	2256 (10)	16314 (11)	73
C(39)	−1142 (10)	6444 (10)	3071 (9)	58	C(80)	4276 (11)	1744 (8)	15449 (11)	63
C(40)	−228 (10)	6488 (9)	3859 (10)	58	C(81)	4450 (11)	2335 (9)	14746 (12)	64
C(41)	−94 (9)	6337 (7)	4862 (9)	42					

[a] Fractional coordinates are ×10^4. [b] Parameters marked by an asterisk were not varied. [c] Isotropic values for those atoms refined anisotropically are calculated by using the formula given by Hamilton: Hamilton W. C. *Acta Crystallogr.* **1959**, *12*, 609.

Table V. Crystallographic Data for $[Y(OSiPh_3)_3[OP(^nBu)_3]_2]$

chem formula	$C_{78}H_{99}O_5P_2Si_3Y$	fw	1351.75
a, Å	13.555 (1)	space group	$P\bar{1}$
b, Å	24.035 (3)	*T*, °C	−156
c, Å	12.780 (1)	λ, Å	0.71069
α, Å	100.87 (0)	ρ_{calcd}, g cm^{-3}	1.211
β, deg	114.51 (0)	μ(Mo Kα), cm^{-1}	9.3
γ, deg	86.05 (0)	*R*	0.0626
V, Å^3	3720.22	R_w	0.0607
Z	2		

positions of the Y atom as well as five oxygen atoms and five P or Si atoms. The remaining non-hydrogen atoms were located in successive difference maps phased with already located atoms. Disorder was observed in two of the *n*-butyl groups on P(77). The disorder was resolved by assigning half-weights to each of the atoms involved. Almost all of the hydrogen atoms were evident in a difference map, except those on the two disordered groups. Hydrogen atoms were idealized (d_{CH} = 0.95 Å) and included in fixed positions for the final cycles of least-squares refinement. All non-hydrogen atoms, (except for the disordered ones) were refined using anisotropic thermal parameters. The final difference map was essentially featureless; the largest peak was 0.86 e/Å^3 in the immediate vicinity of the disorder. The results of the study are shown in Tables VI and VII and Figure 3, which shows only one of the two positions occupied by C(83), C(84), C(87), and C(88) (the γ- and δ-carbons).

Structure Determination of $[Y_2(OSiMe_2{}^tBu)_6(^tBuMe_2SiOH)]$. A suitable crystal was selected from the bulk sample and transferred to the goniostat, where it was cooled to −155 °C for characterization and data collection. A careful search of a limited hemisphere of reciprocal space combined with an automated search of the region from 9 to 12° in 2θ yielded a set of reflections which exhibited monoclinic (2/*m*) symmetry.

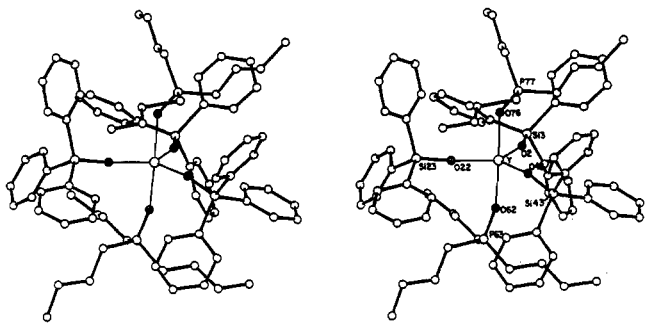

Figure 3. Stereo ORTEP drawing of the non-hydrogen atoms of $[Y(OSiPh_3)_3[OP(^nBu)_3]_2]$, showing selected atom labeling.

Unit cell dimensions were determined from 73 reflections having 2θ between 10 and 29°. The systematic extinctions of 0*k*0 for $k = 2n + 1$ and of *h*0*l* for $l = 2n + 1$ uniquely identified the space group as $P2_1/c$. Data collection[20] ($6° \le 2\theta \le 45°$) was undertaken as detailed in Table VIII of this report. A correction for absorption was carried out. The data contained a large proportion of weak reflections.

The structure was solved by the usual combination of direct methods and Fourier techniques (using the full data set). The Y atoms as well as the O and Si atoms were evident in the best *E* map, and the remainder of the non-hydrogen atoms were located in successive difference Fourier syntheses. During the least-squares refinement process, it became apparent that there was severe disorder in three of the silyloxide ligands (Si(12), Si(44), and Si(52)). These are attached to the more "open" half of the Y_2 molecule: the four-coordinate yttrium. The initial refinement of the occupancies of these three Si atoms converged at very close to 75% for the main atom and 25% for the minor component. The unraveling

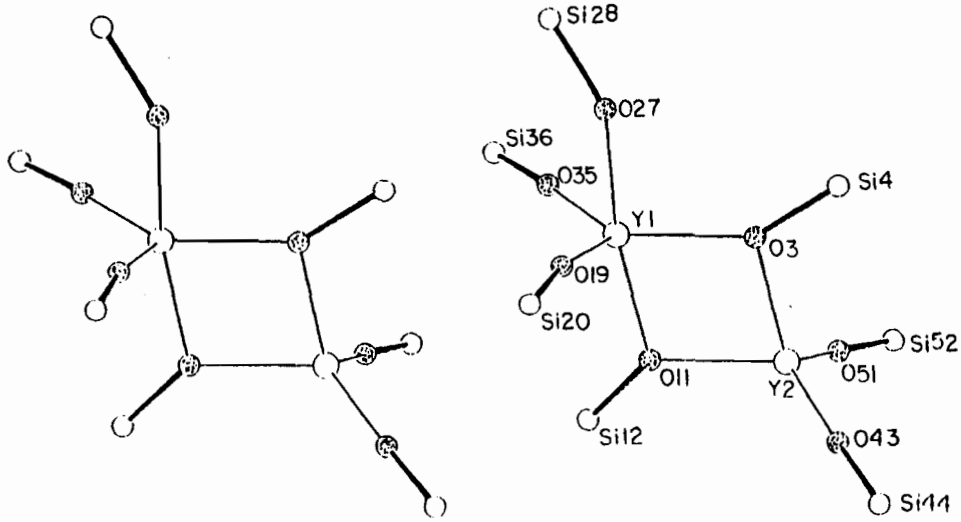

Figure 4. Stereo ORTEP drawing of the $Y_2O_7Si_7$ substructure of $[\{Y(OSiMe_2{}^tBu)_2(HOSiMe_2{}^tBu)\}\{Y(OSiMe_2{}^tBu)\}(\mu\text{-}OSiMe_2{}^tBu)_2]$, showing atom labeling.

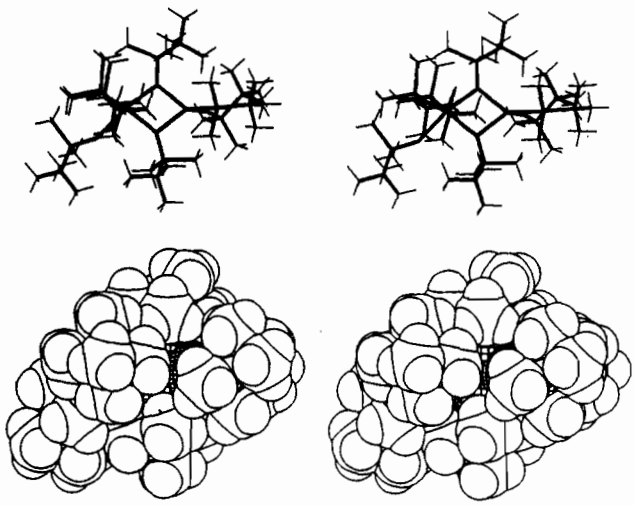

Figure 5. Stereo stick figure and space-filling drawings of $[\{Y(OSiMe_2{}^tBu)_2(HOSiMe_2{}^tBu)\}\{Y(OSiMe_2{}^tBu)\}(\mu\text{-}OSiMe_2{}^tBu)_2]$, with all C–H distances fixed at 1.08 Å. The view is perpendicular to the Y_2O_2 ring.

of the C atoms in the disordered groups proved to be more complex. The least-squares refinement was completed by using anisotropic thermal parameters on the Y atoms and isotropic thermal parameters on all non-hydrogen atoms. Hydrogen atoms were introduced in fixed, calculated positions on the ordered part of the molecule in the hope that it would improve the refinement. The least-squares refinements were carried out by using the 3157 reflections considered observed. The final difference map contained one peak of 1.4 e/Å^3 in one of the disordered groups; the remainder of the peaks were less than 1 e/Å^3.

The results of the structure determination are shown in Tables IX and X and Figures 4 and 5, in which only the disordered atoms of higher (75%) occupancy appear.

X-ray Diffraction Structure Determination of $[K(\eta^2\text{-DME})_3(\eta^1\text{-DME})][Y(OSiPh_3)_4(\eta^2\text{-DME})]$. A crystal of suitable size was mounted under N_2 with silicone grease and then transferred to a goniostat where it was cooled to −144 °C for characterization and data collection.[20] A systematic search of a limited hemisphere of reciprocal space revealed intensities with Laue symmetry and systematic absences consistent with space group $P2_1/n$. This choice was later confirmed by the successful solution of the structure. Following intensity data collection ($6° \le 2\theta \le 45°$), data processing gave a residual of 0.064 for 2899 unique intensities that had been measured more than once. Four standards measured every 300 data showed no significant trends. No correction was made for absorption. Parameters of the unit cell and data collection are shown in Table XI. The structure was solved by a combination of direct methods and Fourier techniques. After the non-hydrogen atoms had been located and partially refined, a difference Fourier map revealed only a few of the hydrogen positions. Hydrogens were therefore included in fixed calculated positions to improve the refinement of the non-hydrogen

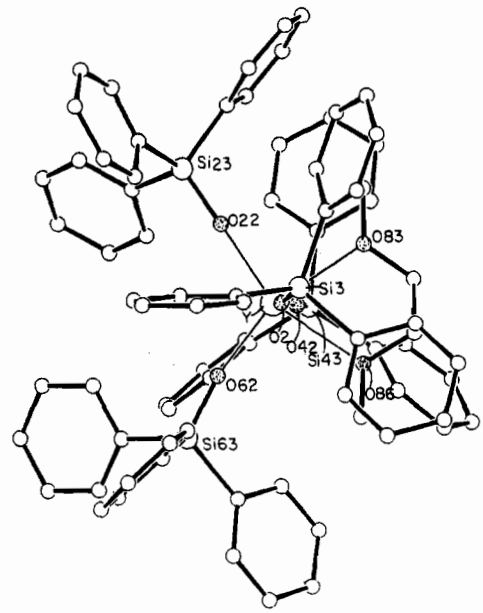

Figure 6. ORTEP drawing of $[Y(OSiPh_3)_4(DME)]^-$, showing selected atom labeling.

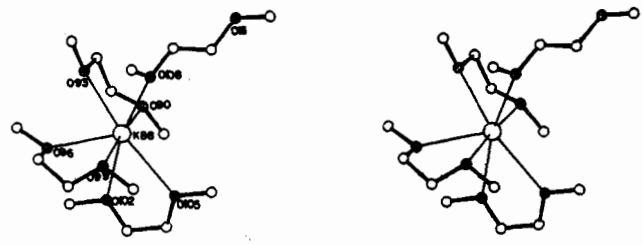

Figure 7. Stereo ORTEP drawing of the non-hydrogen atoms of $[K(DME)_4]^+$, showing selected atom labeling. Carbons (unlabeled) follow the numbering system shown.

atoms, with hydrogen thermal parameters fixed at one plus the isotropic equivalent of the atom to which they were bonded. Non-hydrogen atoms were refined with anisotropic thermal parameters. The final difference map was essentially featureless. There was one peak of 0.75 e/Å^3 in the vicinity of the dangling dimethoxyethane ligand. All other residual peaks were 0.45 e/Å^3 or less. The results of the structure determination are shown in Tables XII and XIII and Figures 6 and 7.

Results

Syntheses. Three equivalents of triphenylsilanol reacted with $[M\{N(SiMe_3)_2\}_3]$ (M = Y, La) in toluene at 0 °C to give high yields of the silyloxide aggregate $[M(OSiPh_3)_3]_n$. These reactions

Table VI. Fractional Coordinates and Isotropic Thermal Parameters[a] for $[Y(OSiPh_3)_3[OP(n\text{-}Bu)_3]_2]$

	10^4x	10^4y	10^4z	$10B_{iso}$, Å^2		10^4x	10^4y	10^4z	$10B_{iso}$, Å^2
Y(1)	2968.7 (4)	2496.2 (2)	2377.4 (4)	14	C(48)	−342 (5)	872 (3)	3171 (6)	42
O(2)	4575 (3)	2278 (1)	2588 (3)	23	C(49)	−68 (5)	1054 (3)	2345 (5)	35
Si(3)	5810 (1)	2371 (1)	2819 (1)	19	C(50)	100 (4)	1353 (2)	−45 (5)	25
C(4)	6770 (4)	1936 (2)	3891 (4)	19	C(51)	−168 (4)	1910 (2)	−167 (5)	28
C(5)	6571 (5)	1356 (2)	3720 (5)	34	C(52)	−1081 (5)	2051 (3)	−1089 (6)	34
C(6)	7301 (5)	1004 (2)	4415 (5)	37	C(53)	−1752 (5)	1641 (3)	−1922 (5)	33
C(7)	8244 (5)	1223 (3)	5310 (5)	32	C(54)	−1509 (5)	1080 (3)	−1829 (5)	40
C(8)	8459 (5)	1786 (3)	5507 (5)	38	C(55)	−607 (5)	937 (2)	−918 (5)	36
C(9)	7735 (5)	2142 (2)	4816 (5)	31	C(56)	2256 (5)	679 (2)	791 (5)	26
C(10)	6014 (4)	2101 (2)	1440 (4)	20	C(57)	1916 (5)	138 (2)	147 (6)	37
C(11)	7041 (4)	2063 (2)	1410 (5)	24	C(58)	2613 (5)	−238 (2)	−152 (6)	40
C(12)	7175 (4)	1836 (2)	395 (5)	25	C(59)	3679 (5)	−84 (3)	203 (6)	39
C(13)	6282 (4)	1635 (2)	−617 (5)	26	C(60)	4035 (5)	450 (3)	845 (5)	37
C(14)	5261 (4)	1661 (2)	−602 (4)	27	C(61)	3341 (5)	825 (2)	1139 (5)	30
C(15)	5134 (4)	1898 (2)	414 (4)	21	O(62)	2476 (3)	2525 (1)	468 (3)	22
C(16)	6205 (4)	3138 (2)	3382 (4)	22	P(63)	2022 (1)	2712 (1)	−698 (1)	20
C(17)	6908 (5)	3428 (2)	3134 (5)	31	C(64)	3084 (4)	2990 (2)	−956 (4)	24
C(18)	7163 (5)	3994 (2)	3585 (5)	35	C(65)	3653 (5)	3514 (3)	−75 (5)	31
C(19)	6714 (5)	4295 (2)	4314 (5)	29	C(66)	4633 (5)	3700 (3)	−219 (5)	32
C(20)	6015 (5)	4028 (3)	4587 (5)	33	C(67)	5107 (5)	4260 (3)	554 (7)	45
C(21)	5761 (5)	3458 (2)	4120 (5)	31	C(68)	1038 (4)	3258 (2)	−787 (5)	24
O(22)	2268 (3)	3307 (1)	2591 (3)	23	C(69)	449 (4)	3436 (2)	−1993 (5)	27
Si(23)	1744 (1)	3898 (1)	2861 (1)	18	C(70)	−249 (5)	3957 (2)	−1978 (5)	31
C(24)	2221 (4)	4460 (2)	2314 (4)	20	C(71)	−926 (5)	4090 (3)	−3181 (5)	38
C(25)	3306 (5)	4634 (2)	2879 (5)	29	C(72)	1372 (4)	2127 (2)	−1850 (4)	24
C(26)	3716 (5)	5010 (3)	2453 (5)	36	C(73)	2078 (4)	1601 (2)	−1832 (5)	26
C(27)	3056 (5)	5225 (2)	1478 (5)	33	C(74)	1462 (5)	1088 (2)	−2694 (5)	29
C(28)	1982 (5)	5059 (2)	900 (5)	32	C(75)	2169 (5)	572 (3)	−2699 (6)	39
C(29)	1572 (4)	4679 (2)	1323 (5)	25	O(76)	3490 (3)	2504 (2)	4310 (3)	29
C(30)	216 (4)	3854 (2)	2117 (4)	22	P(77)	3601 (1)	2139 (1)	5178 (1)	30
C(31)	−271 (5)	3316 (2)	1638 (5)	29	C(78)	4433 (5)	2497 (3)	6621 (5)	38
C(32)	−1403 (5)	3256 (3)	1081 (5)	35	C(79)	5493 (5)	2722 (3)	6638 (5)	43
C(33)	−2057 (4)	3715 (3)	1023 (5)	29	C(80)	6282 (5)	3007 (3)	7795 (6)	43
C(34)	−1594 (4)	4254 (2)	1506 (5)	26	C(81)	7231 (5)	3257 (3)	7700 (6)	44
C(35)	−472 (4)	4322 (2)	2032 (4)	22	C(82)	2290 (6)	1973 (3)	5116 (7)	51 (2)
C(36)	2156 (4)	4111 (2)	4480 (4)	20	C(83)	1620 (10)	2642 (5)	5034 (11)	27 (2)
C(37)	3179 (5)	3961 (2)	5265 (5)	27	C(83)A	1596 (12)	2335 (7)	5295 (13)	46 (3)
C(38)	3516 (5)	4106 (3)	6468 (5)	33	C(84)	405 (11)	2511 (6)	4658 (12)	40 (3)
C(39)	2824 (5)	4401 (2)	6930 (5)	33	C(84)A	992 (13)	2628 (6)	4317 (14)	50 (3)
C(40)	1823 (5)	4550 (3)	6179 (5)	33	C(85)	−66 (7)	3056 (4)	4551 (8)	65 (2)
C(41)	1486 (4)	4409 (2)	4982 (5)	27	C(86)	4230 (6)	1481 (3)	4888 (7)	52 (2)
O(42)	1979 (3)	1775 (1)	1982 (3)	24	C(87)	4273 (11)	1121 (6)	5935 (11)	37 (3)
Si(43)	1345 (1)	1198 (1)	1257 (1)	22	C(87)A	5000 (22)	1093 (12)	5761 (22)	103 (6)
C(44)	880 (4)	871 (2)	2209 (5)	23	C(88)	4449 (16)	681 (8)	5872 (16)	66 (4)
C(45)	1530 (5)	500 (2)	2927 (6)	35	C(88)A	5239 (15)	664 (8)	5971 (16)	64 (4)
C(46)	1257 (6)	327 (3)	3754 (6)	43	C(89)	5219 (7)	305 (4)	6809 (8)	67 (2)
C(47)	336 (6)	516 (3)	3875 (5)	43					

[a] Isotropic values for those atoms refined anisotropically are calculated by using the formula given by Hamilton: Hamilton, W. C. *Acta Crystallogr.* **1959**, *12*, 609.

were complete within several hours, and the $[M(OSiPh_3)_3]_n$ products were isolated as fine featherlike solids free of silanol or amine impurities.[21]

The aggregates $[M(OSiPh_3)_3]_n$ reacted in nearly quantitative yield to form monomeric six-coordinate products *fac*-$[M(OSiPh_3)_3(L)_3]\cdot xL$ (L = THF, x = 1; L = pyridine, x = 0) upon exposure to excess tetrahydrofuran or pyridine, respectively. These complexes were isolated as nicely formed crystalline solids; crystallinity was not degraded upon application of vacuum (ca. 10^{-2} Torr) for several minutes. Monomeric, trigonal-bipyramidal phosphine oxide complexes, $[M(OSiPh_3)_3\{OP(^nBu)_3\}_2]$ were synthesized in excellent yields by treatment of hexane-insoluble $[M(OSiPh_3)_3]_n$ with 2 equiv of $OP(^nBu)_3$ in hexane. The compound $[M(OSiPh_3)_3\{OP(^nBu)_3\}_2]$ was isolated as a well-formed crystalline solid from a chilled, concentrated hexane solution.

The silanol complex $[\{Y(OSiMe_2{}^tBu)_2(HOSiMe_2{}^tBu)\}\{Y(OSiMe_2{}^tBu)_2\}(\mu\text{-}OSiMe_2{}^tBu)_2]$ was prepared in moderate yields directly from $[Y\{N(SiMe_3)_2\}_3]$ and 3.5 equiv of $HOSiMe_2{}^tBu$ in hexane. The product was isolated as a crystalline solid from a minimum of cold alkane. The dinuclear silanol complex was cleaved to *fac*-$[Y(OSiMe_2{}^tBu)_3(THF)_3]$ monomers by treatment with excess tetrahydrofuran; the tetrahydrofuran adduct was isolated as a crystalline solid.

Alkali-metal silyloxide reagents[19] were used to prepare anionic yttrium silyloxide complexes from $[Y(OSiPh_3)_3]_n$. Thus, $[K(\eta^2\text{-DME})_3(\eta^1\text{-DME})][Y(OSiPh_3)_4(\eta^2\text{-DME})]$ was isolated as a crystalline solid from the reaction of $[Y(OSiPh_3)_3]_n$ with $[K(THF)_{0,2}(OSiPh_3)]$ after precipitation from DME/hexane mixtures. A tetrahydrofuran adduct was isolated when the anionic yttrium silyloxide complex precipitated from THF/hexane mixtures. Both the DME adduct and the THF adduct readily lost coordinated Lewis base under a nitrogen stream or upon application of vacuum; the crystallinity of the DME adduct was degraded as a consequence. Toluene-soluble $[K(18\text{-crown-6})][Y(OSiPh_3)_4]$ was isolated from the reaction of $[K(18\text{-crown-6})(OSiPh_3)]$ with $[Y(OSiPh_3)_3]_n$ in toluene as a white powder after trituration of the initially obtained oily residue with pentane. In contrast to these results, $[Li(OSiPh_3)]_n$ did *not* react with $[Y(OSiPh_3)]_n$ in tetrahydrofuran; instead *fac*-$[Y(OSiPh_3)_3(THF)_3]\cdot THF$ was the only Y-containing product isolated.

Solid-State Structures of $[M(OSiPh_3)_3(THF)_3]\cdot THF$. Crystallization of the respective compounds from THF gave isomorphous crystals of $[M(OSiPh_3)_3(THF)_3]\cdot THF$ (M = Y and La)

(21) Similar reactions have been reported previously, but the products were incompletely characterized: Bochkarev, M. N.; Fedorova, E. A.; Radkov, Y. F.; Kazinina, G. S.; Khorshev, S. Y.; Razuvaev, G. A. *Dokl. Akad. Nauk. SSSR* **1984**, *279*, 448.

Table VII. Selected Bond Distances (Å) and Angles (deg) for $[Y(OSiPh_3)_3[OP(^nBu)_3]_2]$

Y(1)–O(2)	2.121 (3)	Si(3)–O(2)	1.598 (4)
Y(1)–O(22)	2.129 (3)	Si(3)–C(4)	1.880 (5)
Y(1)–O(42)	2.118 (3)	Si(3)–C(10)	1.885 (5)
Y(1)–O(62)	2.261 (3)	Si(3)–C(16)	1.877 (5)
Y(1)–O(76)	2.266 (3)	Si(23)–O(22)	1.588 (3)
P(63)–O(62)	1.501 (3)	Si(23)–C(24)	1.893 (5)
P(63)–C(64)	1.801 (5)	Si(23)–C(30)	1.888 (5)
P(63)–C(68)	1.791 (5)	Si(23)–C(36)	1.881 (5)
P(63)–C(72)	1.797 (5)	Si(43)–O(42)	1.594 (4)
P(77)–O(76)	1.495 (4)	Si(43)–C(44)	1.886 (5)
P(77)–C(78)	1.796 (6)	Si(43)–C(50)	1.890 (6)
P(77)–C(82)	1.813 (8)	Si(43)–C(56)	1.886 (6)
P(77)–C(86)	1.796 (8)		
O(2)–Y(1)–O(22)	130.00 (13)	O(2)–Si(3)–C(10)	109.96 (21)
O(2)–Y(1)–O(42)	112.46 (13)	O(2)–Si(3)–C(16)	110.37 (21)
O(2)–Y(1)–O(62)	90.94 (13)	C(4)–Si(3)–C(10)	103.73 (22)
O(2)–Y(1)–O(76)	88.77 (14)	C(4)–Si(3)–C(16)	108.93 (22)
O(22)–Y(1)–O(42)	117.45 (13)	C(10)–Si(3)–C(16)	111.41 (23)
O(22)–Y(1)–O(62)	89.83 (13)	O(22)–Si(23)–C(24)	109.84 (21)
O(22)–Y(1)–O(76)	88.56 (13)	O(22)–Si(23)–C(30)	110.94 (22)
O(42)–Y(1)–O(62)	92.45 (13)	O(22)–Si(23)–C(36)	109.90 (21)
O(42)–Y(1)–O(76)	89.83 (14)	C(24)–Si(23)–C(30)	108.48 (23)
O(62)–Y(1)–O(76)	177.64 (13)	C(24)–Si(23)–C(36)	109.20 (22)
O(62)–P(63)–C(64)	110.42 (22)	C(30)–Si(23)–C(36)	108.44 (22)
O(62)–P(63)–C(68)	112.05 (22)	O(42)–Si(43)–C(44)	109.14 (21)
O(62)–P(63)–C(72)	110.53 (23)	O(42)–Si(43)–C(50)	109.43 (22)
C(64)–P(63)–C(68)	107.19 (25)	O(42)–Si(43)–C(56)	110.69 (22)
C(64)–P(63)–C(72)	108.86 (25)	C(44)–Si(43)–C(50)	107.90 (23)
C(68)–P(63)–C(72)	107.67 (25)	C(44)–Si(43)–C(56)	108.30 (24)
O(76)–P(77)–C(78)	109.35 (26)	C(50)–Si(43)–C(56)	111.32 (24)
O(76)–P(77)–C(82)	111.4 (3)	Y(1)–O(2)–Si(3)	158.09 (22)
O(76)–P(77)–C(86)	110.5 (3)	Y(1)–O(22)–Si(23)	174.57 (22)
C(78)–P(77)–C(82)	109.4 (3)	Y(1)–O(42)–Si(43)	157.83 (22)
C(78)–P(77)–C(86)	108.5 (3)	Y(1)–O(62)–P(63)	162.93 (22)
C(82)–P(77)–C(86)	107.6 (4)	Y(1)–O(76)–P(77)	143.15 (24)
O(2)–Si(3)–C(4)	112.30 (21)		

Table VIII. Crystallographic Data for $[|Y(OSiMe_2{}^tBu)(HOSiMe_2{}^tBu)|\{Y(OSiMe_2{}^tBu)\}(\mu\text{-}OSiMe_2{}^tBu)_2]$

chem formula	$C_{42}H_{106}O_7Si_7Y_2$	space group	$P2_1/c$
a, Å	17.486 (3)	T, °C	−155
b, Å	14.983 (3)	λ, Å	0.71069
c, Å	24.286 (5)	ρ_{calcd}, g cm^{-3}	1.157
β, deg	97.94 (1)	μ(Mo Kα), cm^{-1}	20.1
V, Å^3	1097.71	R	0.111
Z	4	R_w	0.108
fw	1097.71		

in which the metals are six-coordinate. One THF molecule per formula unit is merely trapped in the lattice and does not interact with the metals, which are octahedral and exist exclusively as the facial isomer. A least-squares fit of the two molecules (supplementary material) showed all parts of the molecules (even the lattice solvent) to have identical conformations about all bonds. The major difference was the general expansion of the ligands outward for M = La compared to M = Y. The average least-squares fit (and individual bond length) differences (La minus Y) were 0.131 (0.095) Å for M–$OSiPh_3$ bonds and 0.257 (0.229) Å for M–O(THF) bonds. The larger size of lanthanum than yttrium was thus not reflected equally in the siloxide and ether bond lengths, indicating greater malleability in the weaker bonds to the ether. Oxygen of the coordinated THF is not coplanar with its attached groups. The sum of angles around oxygen range from 357.8 to 358.8° for Y and 353.0 to 358.1° for La. The three $O(C_\alpha)_2$ planes within either complex are mutually orthogonal (Figure 1) and eclipse the axes of the octahedron. This conformation minimizes cis-THF/THF repulsions. Also evident from Figure 1 is the absence of intramolecular graphitic (face-to-face) phenyl stacking. Instead, one Si–C bond from each siloxide is directed along the idealized C_3 axis of the *fac*-$[M(OSiPh_3)_3(THF)_3]$ molecule to form a trigonal prism bounded by the faces of these three phenyl rings. The remaining two phenyl rings per silicon fall into two types, each closely related to the other members of their triplet by an idealized C_3 axis. This is especially evident in Figure 2.

Table IX. Fractional Coordinates[a] and Isotropic Thermal Parameters[b] for $[|Y(OSiMe_2{}^tBu)(HOSiMe_2{}^tBu)|\{Y(OSiMe_2{}^tBu)\}(\mu\text{-}OSiMe_2{}^tBu)_2]$

	x	y	z	$10B_{iso}$, Å^2
Y(1)	2375 (1)	421 (2)	3232 (1)	16
Y(2)	2280 (1)	−1935 (2)	3371 (1)	18
O(3)	3086 (9)	−781 (12)	3562 (7)	21 (4)
Si(4)	3915 (5)	−1064 (5)	3944 (3)	24 (2)
C(5)	3841 (19)	−2286 (23)	4066 (13)	45 (8)
C(6)	4005 (16)	−489 (20)	4621 (12)	35 (7)
C(7)	4738 (18)	−886 (23)	3559 (13)	41 (7)
C(8)	5507 (20)	−1215 (25)	3907 (14)	56 (9)
C(9)	4830 (18)	129 (22)	3482 (13)	42 (7)
C(10)	4618 (20)	−1320 (25)	3001 (15)	56 (9)
O(11)	1572 (9)	−766 (12)	3022 (7)	24 (4)
Si(12)	794 (6)	−779 (8)	2554 (5)	29 (2)
C(13)	386 (22)	404 (29)	2511 (16)	35 (9)
C(14)	945 (23)	−1192 (28)	1824 (16)	38 (9)
C(15)	124 (27)	−1622 (33)	2762 (19)	53 (11)
C(16)	526 (23)	−2521 (29)	2876 (16)	38 (9)
C(17)	−574 (16)	−1785 (20)	2289 (12)	10 (6)
C(18)	−196 (23)	−1277 (29)	3315 (17)	34 (9)
O(19)	1800 (9)	1079 (11)	3821 (7)	23 (4)
Si(20)	1292 (5)	1412 (5)	4290 (3)	24 (2)
C(21)	1409 (20)	2639 (24)	4425 (14)	53 (9)
C(22)	258 (17)	1213 (21)	4074 (12)	39 (7)
C(23)	1608 (16)	797 (21)	4960 (12)	30 (6)
C(24)	1579 (20)	−222 (25)	4862 (14)	56 (9)
C(25)	2460 (16)	1057 (19)	5183 (12)	31 (7)
C(26)	1129 (19)	1026 (23)	5385 (14)	49 (8)
O(27)	3262 (10)	1546 (12)	3730 (7)	25 (4)
Si(28)	3664 (4)	2526 (5)	3575 (3)	22 (2)
C(29)	2840 (16)	3288 (20)	3355 (12)	33 (7)
C(30)	4197 (17)	2302 (20)	3009 (12)	35 (7)
C(31)	4291 (16)	2944 (21)	4222 (12)	33 (6)
C(32)	3856 (19)	3047 (25)	4701 (14)	53 (8)
C(33)	4631 (24)	3834 (29)	4068 (17)	75 (11)
C(34)	4934 (18)	2325 (22)	4388 (13)	42 (7)
O(35)	2435 (10)	955 (12)	2452 (7)	25 (4)
Si(36)	2430 (4)	1320 (6)	1816 (3)	25 (2)
C(37)	2693 (19)	2519 (22)	1789 (13)	43 (7)
C(38)	1451 (14)	1198 (18)	1417 (10)	20 (5)
C(39)	3149 (16)	656 (20)	1457 (12)	29 (6)
C(40)	3005 (17)	−291 (22)	1472 (12)	39 (7)
C(41)	3962 (18)	776 (23)	1752 (13)	42 (7)
C(42)	3153 (20)	1016 (24)	865 (14)	54 (9)
O(43)	1902 (11)	−2529 (13)	4050 (8)	33 (4)
Si(44)	1601 (6)	−3011 (8)	4597 (4)	26 (2)
C(45)	2340 (22)	−2725 (26)	5242 (16)	33 (9)
C(46)	601 (20)	−2651 (25)	4711 (15)	28 (8)
C(47)	1527 (23)	−4280 (30)	4448 (17)	40 (9)
C(48)	933 (22)	−4476 (27)	3959 (15)	34 (9)
C(49)	1220 (20)	−4753 (24)	4980 (14)	24 (8)
C(50)	2422 (22)	−4556 (28)	4363 (16)	37 (9)
O(51)	2645 (11)	−2759 (14)	2789 (8)	41 (5)
Si(52)	3089 (7)	−3402 (8)	2381 (5)	32 (3)
C(53)	3472 (16)	−2787 (20)	1786 (12)	8 (6)
C(54)	3908 (25)	−4017 (31)	2818 (18)	46 (10)
C(55)	2355 (26)	−4225 (34)	2063 (20)	54 (11)
C(56)	2740 (26)	−4980 (30)	1701 (18)	42 (10)
C(57)	1698 (26)	−3787 (33)	1627 (19)	49 (10)
C(58)	1998 (22)	−4756 (26)	2493 (16)	21 (9)
Si(12)1	575 (13)	−719 (17)	2910 (10)	0 (4)
C(13)1	421 (72)	515 (93)	2708 (54)	27 (19)
C(14)1	159 (47)	−1002 (54)	3585 (34)	0 (14)
Si(44)1	2010 (26)	−3395 (31)	4510 (18)	50 (10)
Si(52)1	2765 (15)	−3841 (19)	2545 (10)	5 (5)
C(53)1	2802 (54)	−3546 (67)	1772 (40)	19 (16)
C(55)1	3756 (49)	−4376 (62)	2878 (35)	0 (14)
C(56)1	1887 (60)	−4459 (74)	2639 (45)	16 (18)
C(57)1	2013 (48)	−3307 (56)	1496 (34)	3 (14)
C(58)1	3017 (91)	−4459 (113)	1472 (66)	73 (20)

[a] Fractional coordinates are ×10^4. [b] Isotropic values for those atoms refined anisotropically are calculated by using the formula given by Hamilton: Hamilton, W. C. *Acta Crystallogr.* **1959**, *12*, 609.

The M–O(Si) distances are quite short in $[M(OSiPh_3)_3(THF)_3]$. While the O–Si distances do not differ significantly,

Table X. Selected Bond Distances (Å) and Angles (deg) for $[\{Y(OSiMe_2{}^tBu)(HOSiMe_2{}^tBu)\}\{Y(OSiMe_2{}^tBu)(\mu\text{-}OSiMe_2{}^tBu)_2]$

Y(1)–O(3)	2.271 (17)	Y(2)–O(3)	2.239 (17)
Y(1)–O(11)	2.280 (17)	Y(2)–O(11)	2.242 (18)
Y(1)–O(19)	2.104 (17)	Y(2)–O(43)	2.060 (19)
Y(1)–O(27)	2.487 (18)	Y(2)–O(51)	2.046 (20)
Y(1)–O(35)	2.072 (17)		
O(3)–Y(1)–O(11)	75.5 (6)	O(11)–Y(2)–O(51)	114.7 (7)
O(3)–Y(1)–O(19)	114.9 (6)	O(43)–Y(2)–O(51)	117.3 (8)
O(3)–Y(1)–O(27)	95.3 (6)	Y(1)–O(3)–Y(2)	103.9 (6)
O(3)–Y(1)–O(35)	122.4 (6)	Y(1)–O(3)–Si(4)	142.3 (10)
O(11)–Y(1)–O(19)	100.3 (6)	Y(2)–O(3)–Si(4)	113.2 (9)
O(11)–Y(1)–O(27)	164 (3)	Y(1)–O(11)–Y(2)	103.5 (6)
O(11)–Y(1)–O(35)	101.8 (6)	Y(1)–O(11)–Si(12)	126.0 (11)
O(19)–Y(1)–O(35)	122.0 (7)	Y(2)–O(11)–Si(12)	127.7 (11)
O(19)–Y(1)–O(27)	71.1 (7)	Y(1)–O(19)–Si(20)	169.8 (11)
O(27)–Y(1)–O(35)	94.4 (6)	Y(1)–O(27)–Si(28)	136.9 (11)
O(3)–Y(2)–O(11)	76.9 (6)	Y(1)–O(35)–Si(36)	175.5 (11)
O(3)–Y(2)–O(43)	115.5 (7)	Y(2)–O(43)–Si(44)	179.7 (13)
O(3)–Y(2)–O(51)	111.2 (7)	Y(2)–O(51)–Si(52)	170.1 (13)
O(11)–Y(2)–O(43)	114.8 (7)		

Table XI. Crystallographic Data for $[K(DME)_4][Y(OSiPh_3)_4(DME)]$

chem formula	$C_{92}H_{110}KO_{14}Si_4Y$	space group	$P2_1/n$
a, Å	14.545 (3)	T, °C	−144
b, Å	29.865 (6)	λ, Å	0.71069
c, Å	21.726 (4)	ρ_{calcd}, g cm^{-3}	1.241
β, deg	107.61 (1)	μ(Mo Kα), cm^{-1}	8.07
V, Å^3	8995.69	R	0.0654
Z	4	R_w	0.0616
fw	1680.22		

the M–O–Si angles vary by 4° (M = Y) and 9° (M = La), but with no consistent correlation to the M–O bond lengths.

The fact that the fourth THF molecule in the solid material does *not* coordinate to either metal indicates steric saturation of the metal at coordination number 6 for this ligand set. This conclusion has consequences for the mechanism of THF ligand exchange (see below).

Solid-State Structure of $[Y(SiPh_3)_3\{OP(^nBu)_3\}_2]$. The molecule adopts, to a close approximation, a trigonal-bipyramidal geometry, with both phosphine oxides axial. Axial/equatorial angles are 88.56–92.45° with the phosphine oxides 177.64° apart. Angles between siloxide oxygens deviate somewhat from the 120° ideal (117.45 (13)–130.00 (13)°). Bond lengths to the equatorial (siloxide) oxygens are statistically identical, and shorter than those to the (mutually equivalent) oxygens of $OP(^nBu)_3$. While the siloxide O–Y distance is shorter than the phosphine oxide O–Y distance, the Si–O distance is longer than the P–O distance.

The Y–O–Si angles span a considerable range (157.83–174.57°), and the phosphine oxides are even more malleable (Y–O–P angles of 143.15 and 162.93°). Throughout these deformations, the angles at the tetrahedral silicon and phosphorus are all within the 3° of 109°.

The phenyl rings are arranged so that one phenyl on each silicon lies approximately in the equatorial plane, and these three phenyl rings are arranged in phase (i.e., they are directed in the same "sense") around the O(2)O(22)O(42) plane. This gives efficient cogging of these three $OSiPh_3$ groups, and directs the remaining six phenyl groups toward the $OP(^nBu)_3$ groups. As a result, the $OP(^nBu)_3$ 3-fold rotors are approximately staggered with respect to the YO(2)O(22)O(42) rotor but the butyl groups eclipse the in-plane phenyl ring. Only one of the three ^{n}Bu groups on each phosphorus is swept back away from the P–O–Y region to give a conical form; the other two sweep outward from the pseudo-C_3 axis, into the space created by the phenyl rings.

Solid-State Structure of $[\{(OSiMe_2{}^tBu)_2(HOSiMe_2{}^tBu)\}\{Y(OSiMe_2{}^tBu)_2\}(\mu\text{-}OSiMe_2{}^tBu)_2]$. The molecule $[\{Y(OSiMe_2{}^tBu)_2(HOSiMe_2{}^tBu)\}\{Y(OSiMe_2{}^tBu)_2\}(\mu\text{-}OSiMe_2{}^tBu)_2]$ is comprised of two yttrium centers linked by two bridging siloxides. Noteworthy is the asymmetry of the compound, due to the coordination of only one silan*ol* molecule in a terminal site (on Y(1)). One yttrium is thus four-coordinate and the second is five-coordinate, and all Y–O (silyloxide) distances are slightly (~0.04 Å) shorter to the four-coordinate metal. The former (Y(2)) is approximately tetrahedral while the latter (Y(1)) is approximately trigonal bipyramidal. In this trigonal bipyramid, the silanol (O(27)) and one μ-silyloxide (O(11)) are the axial groups. As a result of the binding of silanol, the closest μ-silyloxide silicon (Si(4)) bends away from the alcohol (O(27)). Nevertheless, there is no evidence for intramolecular hydrogen bonding involving the silanol proton. This conclusion is reinforced by the relatively high ν(OH) frequency (vide infra). The terminal silyloxides are all nearly linear at oxygen (169.8 (11)–179.7 (13)°), while the silanol was readily identifiable not only by its long Y–O bond (0.4 Å longer than to terminal silyloxides on Y(1)) but also by its strongly bent angle (136.9°) at oxygen.

The question arises as to why silanol coordinates to only one yttrium in this compound. The Y/Y separation (3.552 (4) Å) is nonbonding, and the Y–O–Y angles at the bridging alkoxides are obtuse (103.9 (6) and 103.5 (6)°). Nevertheless, the binding of alcohol to one Y has its influence on the second metal center. This cannot be perceived from Figure 4, but requires consideration of the ^{t}Bu and methyl groups. As is evident in Figure 5, the silyl group of one μ-siloxide leans away from the five-coordinate metal. In addition, methyl groups from *both* μ-siloxides shield the two sides of the four-coordinate metal. In this way, the structure of $Y_2(OSiMe_2{}^tBu)_6(^tBuMe_2SiOH)_n$ for $n = 1$ may foreshadow excessive congestion when $n = 2$. The stereo stick figure in Figure 5 shows how the hydroxyl proton is embedded in the hydrocarbon moiety of the μ-siloxide, and also shows the steric shielding of both metals by an aliphatic exterior in $[\{Y(OSiMe_2{}^tBu)_2(HOSiMe_2{}^tBu)\}\{Y(OSiMe_2{}^tBu)_2\}(\mu\text{-}OSiMe_2{}^tBu)_2]$.

Solid-State Structure of $[K(\eta^2\text{-DME})_3(\eta^1\text{-DME})][Y(OSiPh_3)_4(\eta^2\text{-DME})]$. Potassium has a coordination number of 7, due to three η^2-DME ligands and one η^1-DME ligand. The coordination geometry can only be described as irregular. There are two transoid (O–K–O angles of 176.57 (22) and 169.59 (20)°) sets of oxygens, but the three oxygens out of that KO_4 plane describe no regular polyhedron. Two of the η^2-DME ligands display a short/long pattern of K/O distances, but the third DME does not. The η^1-DME displays (2.757 (7) Å) neither the longest (2.809 (7) Å) nor the shortest (2.710 (7) Å) K–O distance. All η^2-DME ligands, including that on Y, adopt puckered *rac*-conformations, with very small O–M–O chelate "bite" angles: 58.69 (19)–61.18 (21)° for K and 66.52 (17)° for Y.

The coordination geometry of yttrium is pseudooctahedral, and the small DME bite angle permits the bulky $OSiPh_3$ ligands to lean toward DME: the cis O(22)–Y–O(62) angle opens to 108.43 (20)° and the trans O(2)–Y–O(42) angle closes (toward DME) to 160.43 (18)°. The mutually trans siloxide Y–O distances (mean value 2.194 (5) Å) are distinctly longer than those mutually cis (mean value 2.145 (5) Å). This originates in the long (mean value 2.509 (5) Å) Y–O bonds to DME. The DME oxygens on Y are distinctly pyramidal (angles sum to 341 and 346°), and the methyl substituents adopt a trans diequatorial conformation in the five-membered ring. All four Si–O distances are equal, and the Y–O–Si angles vary (163.7 (3)–175.1 (3)°, but with no consistent pattern. There is *no* graphitic (face-to-face) stacking among the 12 rings within one anion, but several of these rings are oriented to present a ring face to the DME also bound to yttrium. Trans to this DME, in the open angle O(22)–Y–O(62), the phenyl rings rotate to form a nest or basket for the $K(DME)_4^+$ cation. This presumably shows a favorable conformation for an ion pair. The structure of the anion is very similar to that of $Ce(OSiPh_3)_4(\eta^2\text{-DME})$.[22]

NMR Spectral Properties. The hydrogen-1 NMR spectra of $[M(OSiPh_3)_3]_n$ (M = Y, La) showed broad, complex patterns between 7.5 and 6.5 ppm. No resonances outside the phenyl region were detected. Carbon-13 NMR spectra were similarly complex between 135.4 and 127.6 ppm. These compounds were too in-

(22) Gradeff, P. S.; Yunlu, K.; Gleizes, A.; Galy, J. *Polyhedron* **1989**, *8*, 1001.

Table XII. Fractional Coordinates[a] and Isotropic Thermal Parameters[b] for $[K(DME)_4][Y(OSiPh_3)_4(DME)]$

	x	y	z	$10B_{iso}$, Å^2		x	y	z	$10B_{iso}$, Å^2
Y(1)	6679 (1)	5920.7 (3)	6811.9 (3)	12	C(57)	7713 (6)	6585 (3)	5152 (4)	26
O(2)	5201 (3)	5817 (2)	6841 (2)	17	C(58)	7506 (6)	6818 (3)	4571 (4)	27
Si(3)	4157 (2)	5619 (1)	6747 (1)	15	C(59)	8136 (8)	6800 (3)	4207 (4)	37
C(4)	3211 (5)	5912 (3)	6067 (3)	17	C(60)	8974 (7)	6542 (3)	4434 (4)	33
C(5)	2892 (6)	6336 (3)	6162 (4)	24	C(61)	9182 (6)	6317 (3)	5010 (4)	26
C(6)	2276 (7)	6578 (3)	5659 (4)	30	O(62)	6923 (4)	6546 (2)	7325 (2)	19
C(7)	1962 (6)	6394 (3)	5048 (4)	31	Si(63)	6940 (2)	7043 (1)	7583 (1)	16
C(8)	2273 (6)	5971 (3)	4945 (4)	30	C(64)	5907 (5)	7145 (3)	7933 (3)	14
C(9)	2885 (6)	5726 (3)	5448 (4)	23	C(65)	5103 (5)	6868 (3)	7744 (4)	18
C(10)	4078 (6)	5006 (3)	6558 (3)	17	C(66)	4334 (6)	6923 (3)	7994 (4)	24
C(11)	4919 (6)	4749 (3)	6669 (4)	20	C(67)	4368 (6)	7255 (3)	8427 (4)	25
C(12)	4880 (6)	4291 (3)	6531 (4)	22	C(68)	5162 (7)	7533 (3)	8627 (4)	27
C(13)	4007 (6)	4081 (3)	6284 (4)	23	C(69)	5935 (6)	7477 (3)	8385 (4)	21
C(14)	3160 (6)	4324 (3)	6168 (4)	22	C(70)	8081 (5)	7171 (3)	8246 (4)	19
C(15)	3205 (5)	4770 (3)	6312 (4)	18	C(71)	8639 (5)	6827 (3)	8610 (4)	19
C(16)	3767 (5)	5703 (3)	7496 (4)	19	C(72)	9468 (6)	6914 (3)	9127 (4)	27
C(17)	2806 (6)	5680 (3)	7484 (4)	29	C(73)	9770 (7)	7349 (4)	9277 (5)	38
C(18)	2536 (6)	5726 (4)	8036 (4)	35	C(74)	9236 (6)	7694 (3)	8927 (5)	33
C(19)	3220 (6)	5804 (3)	8617 (4)	29	C(75)	8415 (6)	7599 (3)	8410 (4)	28
C(20)	4171 (6)	5836 (3)	8648 (4)	27	C(76)	6830 (5)	7468 (3)	6919 (3)	15
C(21)	4448 (6)	5789 (3)	8093 (4)	22	C(77)	6417 (6)	7889 (3)	6915 (4)	27
O(22)	7273 (4)	5393 (2)	7483 (3)	21	C(78)	6372 (7)	8206 (3)	6432 (4)	30
Si(23)	7924 (2)	5044 (1)	7967 (1)	20	C(79)	6723 (6)	8090 (3)	5926 (4)	25
C(24)	8159 (6)	4528 (3)	7531 (4)	24	C(80)	7097 (6)	7674 (3)	5904 (4)	28
C(25)	8917 (7)	4496 (3)	7269 (4)	30	C(81)	7177 (6)	7361 (3)	6404 (4)	27
C(26)	9002 (8)	4124 (3)	6917 (4)	41	C(82)	6798 (6)	4985 (3)	5939 (4)	21
C(27)	8325 (10)	3781 (3)	6799 (5)	54	O(83)	6217 (3)	5377 (2)	5890 (2)	16
C(28)	7580 (10)	3822 (3)	7045 (5)	52	C(84)	6050 (6)	5592 (3)	5276 (4)	21
C(29)	7482 (7)	4180 (3)	7404 (4)	39	C(85)	5354 (6)	5965 (3)	5238 (4)	27
C(30)	7339 (6)	4823 (3)	8568 (4)	24	O(86)	5769 (4)	6275 (2)	5754 (2)	17
C(31)	7620 (6)	4443 (3)	8949 (4)	25	C(87)	5141 (6)	6641 (3)	5748 (4)	23
C(32)	7174 (6)	4300 (3)	9372 (4)	30	K(88)	6898 (2)	6459 (1)	10863 (1)	31
C(33)	6387 (8)	4533 (4)	9438 (5)	44	C(89)	6369 (12)	5312 (4)	10595 (7)	81
C(34)	6057 (8)	4899 (4)	9051 (6)	54	O(90)	6123 (6)	5651 (3)	10991 (4)	60
C(35)	6545 (8)	5044 (3)	8623 (5)	43	C(91)	6319 (10)	5527 (4)	11627 (6)	64
C(36)	9106 (6)	5312 (3)	8422 (4)	19	C(92)	5851 (11)	5848 (4)	11950 (5)	69
C(37)	9678 (6)	5169 (3)	9023 (4)	24	O(93)	6264 (8)	6289 (3)	11920 (4)	76
C(38)	10542 (6)	5386 (3)	9344 (4)	24	C(94)	5848 (15)	6625 (5)	12192 (7)	105
C(39)	10853 (6)	5748 (3)	9070 (4)	25	C(95)	8451 (13)	6689 (5)	12505 (6)	96
C(40)	10299 (6)	5897 (3)	8481 (4)	23	O(96)	8355 (6)	6792 (2)	11852 (3)	56
C(41)	9432 (6)	5684 (3)	8151 (4)	21	C(97)	8675 (7)	7229 (4)	11781 (5)	51
O(42)	7904 (3)	6006 (2)	6430 (2)	18	C(98)	8693 (7)	7299 (4)	11117 (6)	49
Si(43)	8845 (2)	6063 (1)	6215 (1)	19	O(99)	7750 (4)	7262 (2)	10687 (3)	34
C(44)	9482 (5)	5526 (3)	6174 (4)	20	C(100)	7706 (9)	7369 (4)	10037 (5)	51
C(45)	9184 (6)	5237 (3)	5630 (4)	28	C(101)	9172 (8)	5828 (4)	11489 (5)	61
C(46)	9650 (8)	4839 (3)	5608 (5)	41	O(102)	8489 (5)	5918 (3)	10891 (3)	56
C(47)	10434 (7)	4706 (3)	6115 (6)	44	C(103)	8773 (11)	5901 (5)	10375 (6)	89
C(48)	10747 (7)	4978 (3)	6644 (5)	39	C(104)	8076 (7)	5969 (4)	9755 (5)	43
C(49)	10281 (6)	5374 (3)	6682 (4)	26	O(105)	7304 (6)	6224 (3)	9734 (3)	62
C(50)	9738 (6)	6453 (3)	6768 (4)	20	C(106)	6647 (7)	6313 (4)	9145 (5)	52
C(51)	9475 (6)	6733 (3)	7193 (4)	22	C(107)	5378 (7)	7448 (4)	10778 (5)	48
C(52)	10101 (6)	7043 (3)	7570 (4)	22	O(108)	5275 (4)	6991 (2)	10597 (3)	46
C(53)	11031 (6)	7081 (3)	7533 (4)	26	C(109)	4351 (8)	6794 (5)	10484 (5)	67
C(54)	11321 (6)	6809 (3)	7119 (4)	27	C(110)	3783 (7)	6835 (5)	9861 (5)	60
C(55)	10699 (6)	6497 (3)	6736 (4)	24	O(111)	2817 (4)	6662 (2)	9731 (3)	33
C(56)	8561 (6)	6333 (3)	5396 (4)	21	C(112)	2214 (7)	6818 (3)	9135 (5)	35

[a] Fractional coordinates are $\times 10^4$. [b] Isotropic values for those atoms refined anisotropically are calculated using the formula given by Hamilton: Hamilton, W. C. *Acta Crystallogr.* **1959**, *12*, 609.

soluble in any unreactive solvent to obtain ^{29}Si NMR data.

In contrast, in the ^1H NMR spectra of the adducts $[M(OSiPh_3)_3L_n]\cdot xL$ {M = Y, La, L = THF, $n = 3$, $x = 1$; L = py, $n = 3$, $x = 0$; L = $OP(^nBu)_3$, $n = 2$, $x = 0$}, simple monosubstituted aromatic patterns (ortho doublet, para triplet, meta triplet) were observed along with resonances expected for the Lewis base ligands. Integration of the ^1H spectra permitted determination of $-OSiPh_3$ to L stoichiometry. Carbon-13 NMR spectra were as expected based on the ^1H data, revealing simple, four-peak patterns in the phenyl region. The complexes *trans*-$[M(OSiPh_3)_3\{OP(^nBu)_3\}_2]$ (M = Y, La) gave rise to ^{31}P NMR resonances at 58.2 and 57.6 ppm, respectively. For the yttrium complex a two-bond ^{89}Y–^{31}P coupling constant of 7.4 Hz was resolved.

Both the hydrogen-1 and carbon-13 NMR spectra for the silanol complex $[\{Y(OSiMe_2{}^tBu)_2(HOSiMe_2{}^tBu)\}\{Y(OSiMe_2{}^tBu)_2\}(\mu\text{-}OSiMe_2{}^tBu)_2]$ were unexpectedly simple, showing resonances for only one type of $-OSiMe_2{}^tBu$ group. The silanol hydroxyl hydrogen resonance was detected at 1.64 ppm with the anticipated integrated intensity.

The THF adduct $[Y(OSiMe_2{}^tBu)_3(THF)_3]$, showed resonances for only one type of $-OSiMe_2{}^tBu$ group along with peaks associated with coordinated tetrahydrofuran. At −90 °C in CD_2Cl_2, however, two sets of $-OSiMe_2{}^tBu$-based ^1H NMR resonances were detected along with resonances for both coordinated and free tetrahydrofuran. This low-temperature result indicated that $[Y(OSiMe_2{}^tBu)_3(THF)_3]$ participates in a dynamic equilibrium involving a partially desolvated Y-complex and free THF. In chloroform-*d*, the resonances for bound THF appeared downfield of the analogous resonances for the free ligand; in contrast the signals for coordinated THF in $[M(OSiPh_3)_3(THF)_3]\cdot THF$ (M = Y, La) in $CDCl_3$ resonated upfield of those for the free ligand. Some influence of the phenyl ring currents is thus likely.

Table XIII. Selected Bond Distances (Å) and Angles (deg) for $[K(DME)_4][Y(OSiPh_3)_4(DME)]$

Y(1)–O(2)	2.192 (5)	Si(3)–C(10)	1.875 (8)
Y(1)–O(22)	2.143 (5)	Si(3)–C(16)	1.894 (8)
Y(1)–O(42)	2.196 (5)	Si(23)–O(22)	1.577 (6)
Y(1)–O(62)	2.147 (5)	Si(23)–C(24)	1.894 (9)
Y(1)–O(83)	2.506 (5)	Si(23)–C(30)	1.882 (9)
Y(1)–O(86)	2.512 (5)	Si(23)–C(36)	1.883 (8)
K(88)–O(90)	2.715 (7)	Si(43)–O(42)	1.584 (5)
K(88)–O(93)	2.768 (8)	Si(43)–C(44)	1.868 (8)
K(88)–O(96)	2.710 (7)	Si(43)–C(50)	1.881 (8)
K(88)–O(99)	2.779 (6)	Si(43)–C(56)	1.883 (9)
K(88)–O(102)	2.809 (7)	Si(63)–O(62)	1.585 (6)
K(88)–O(105)	2.782 (7)	Si(63)–C(64)	1.902 (8)
K(88)–O(108)	2.757 (7)	Si(63)–C(70)	1.880 (8)
Si(3)–O(2)	1.584 (5)	Si(63)–C(76)	1.891 (8)
Si(3)–C(4)	1.900 (8)		
O(2)–Y(1)–O(22)	94.21 (19)	O(102)–K(88)–O(108)	169.59 (20)
O(2)–Y(1)–O(42)	160.43 (18)	O(105)–K(88)–O(108)	110.90 (21)
O(2)–Y(1)–O(62)	96.76 (19)	Y(1)–O(2)–Si(3)	163.7 (3)
O(2)–Y(1)–O(83)	84.45 (17)	Y(1)–O(22)–Si(23)	167.6 (3)
O(2)–Y(1)–O(86)	80.57 (17)	Y(1)–O(42)–Si(43)	175.1 (3)
O(22)–Y(1)–O(42)	97.84 (19)	Y(1)–O(62)–Si(63)	168.6 (3)
O(22)–Y(1)–O(62)	108.43 (20)	Y(1)–O(83)–C(82)	117.5 (4)
O(22)–Y(1)–O(83)	91.35 (19)	Y(1)–O(83)–C(84)	112.5 (4)
O(22)–Y(1)–O(86)	157.57 (19)	C(82)–O(83)–C(84)	111.4 (6)
O(42)–Y(1)–O(62)	94.00 (19)	Y(1)–O(86)–C(85)	115.0 (4)
O(42)–Y(1)–O(83)	79.91 (17)	Y(1)–O(86)–C(87)	119.3 (4)
O(42)–Y(1)–O(86)	82.43 (17)	C(85)–O(86)–C(87)	111.8 (6)
O(62)–Y(1)–O(83)	159.99 (18)	K(88)–O(90)–C(89)	112.2 (6)
O(62)–Y(1)–O(86)	93.89 (18)	K(88)–O(90)–C(91)	112.0 (7)
O(83)–Y(1)–O(86)	66.52 (17)	C(89)–O(90)–C(91)	113.4 (10)
O(90)–K(88)–O(93)	59.97 (23)	K(88)–O(93)–C(92)	116.6 (6)
O(90)–K(88)–O(96)	119.67 (25)	K(88)–O(93)–C(94)	121.2 (7)
O(90)–K(88)–O(99)	176.57 (22)	C(92)–O(93)–C(94)	113.1 (11)
O(90)–K(88)–O(102)	81.40 (26)	K(88)–O(96)–C(95)	122.0 (8)
O(90)–K(88)–O(105)	94.08 (25)	K(88)–O(96)–C(97)	117.2 (6)
O(90)–K(88)–O(108)	100.23 (24)	C(95)–O(96)–C(97)	112.1 (9)
O(93)–K(88)–O(96)	77.67 (26)	K(88)–O(99)–C(98)	111.2 (6)
O(93)–K(88)–O(99)	123.14 (22)	K(88)–O(99)–C(100)	116.0 (6)
O(93)–K(88)–O(102)	110.83 (27)	C(98)–O(99)–C(100)	112.3 (8)
O(93)–K(88)–O(105)	153.96 (25)	K(88)–O(102)–C(101)	118.5 (6)
O(93)–K(88)–O(108)	78.50 (27)	K(88)–O(102)–C(103)	118.5 (7)
O(96)–K(88)–O(99)	61.18 (21)	C(101)–O(102)–C(103)	117.9 (9)
O(96)–K(88)–O(102)	75.66 (23)	K(88)–O(105)–C(104)	120.7 (6)
O(96)–K(88)–O(105)	117.89 (26)	K(88)–O(105)–C(106)	120.0 (6)
O(96)–K(88)–O(108)	111.74 (22)	C(104)–O(105)–C(106)	118.7 (8)
O(99)–K(88)–O(102)	95.80 (23)	K(88)–O(108)–C(107)	119.0 (5)
O(99)–K(88)–O(105)	82.74 (23)	K(88)–O(108)–C(109)	120.3 (8)
O(99)–K(88)–O(108)	82.17 (20)	C(107)–O(108)–C(109)	117.5 (9)
O(102)–K(88)–O(105)	58.69 (19)	C(110)–O(111)–C(112)	111.1 (7)

At ambient temperature, the ^1H and ^{13}C NMR spectra of the anionic yttrium silyloxide complex $[K(\eta^2\text{-DME})_3(\eta^1\text{-DME})][Y(OSiPh_3)_4(\eta^2\text{-DME})]$ revealed a simple phenyl pattern and resonances for only one type of DME ligand. Variable-temperature ^1H NMR experiments revealed that **11** is fluxional in solution. As sample temperature was reduced, the DME region broadened and finally (around −50 °C) resolved into two sets of DME-based signals (K-coordinated and Y-coordinated). At this temperature, only a simple phenyl pattern was detected. When the sample was cooled further, the DME-based signals remained unchanged, but signals in the phenyl region broadened, and near −90 °C resolved into two sets (–$OSiPh_3$ cis to DME, and –$OSiPh_3$ trans to DME).

The NMR data for $[K(18\text{-crown-6})][Y(OSiPh_3)_4]$ were likewise straightforward. Integration of the hydrogen-1 spectra established the K(18-crown-6) to –$OSiPh_3$ ratio of 1:4. Low-temperature ^1H NMR spectra are not available in noncoordinating solvents due to low solubility.

Infrared Spectral Properties. All complexes reported here bearing the –$OSiPh_3$ ligand shared a set of infrared active absorptions, namely aromatic ν(CH) modes near 3030 cm^{-1} and monosubstituted aromatic overtone patterns between 1950 and 1780 cm^{-1}. Additionally, intense bands between 1100 and 950 cm^{-1} were detected in each spectrum and were attributed to ν(OSi) modes. No high energy ν(OH) or ν(NH) bands were observed in any (triphenylsilyl)oxide complex. Complexes containing the –$OSiMe_2{}^tBu$ ligand gave rise to intense absorptions near 1240 cm^{-1}, assigned as $\delta_s(SiCH_3)$ modes, as well as very intense absorptions between 1050 and 950 cm^{-1} assigned as ν(SiO) modes. The infrared spectrum of the silanol complex $[\{Y(OSiMe_2{}^tBu)_2(HOSiMe_2{}^tBu)\}\{Y(OSiMe_2{}^tBu)(\mu\text{-}OSiMe_2{}^tBu)\}_2]$ revealed a broad, shallow band at 3320 cm^{-1}, which was assigned as a ν(OH) mode.

Discussion

Syntheses and Preparative Strategies. Reaction of $[M\{N(SiMe_3)_2\}_3]$ (M = Y, La) with 3 equiv of Ph_3SiOH provided a convenient route to homoleptic yttrium/lanthanum silyloxide complexes $[M(OSiPh_3)_3]_n$ (M = Y (1), La (2)), which can be isolated as white, featherlike solids. Unfortunately, it was not possible to obtain either of these complexes in a form suitable for X-ray analysis, so definitive structural assignments have not been possible. However, because of the broad and complicated appearance of the hydrogen-1 and carbon-13 NMR spectra in the phenyl region, we have postulated that **1** and **2** are aggregates held together with bridging –$OSiPh_3$ groups. Efforts to support this hypothesis by using ^{29}Si NMR have failed owing to limited solubility in solvents with which these compounds do not react.

Because the $[M\{N(SiMe_3)_2\}_3]$ reagent is alkane- and arene-soluble, the product silyloxide complexes are formed without complications from Lewis basic solvent coordination. Such complications often attend preparative routes based on metal halide/alkali-metal alkoxide salt metathesis because reagent solubilities are too low in noncoordinating solvents. As regards the long-range goal of developing polymetallic silyloxide aggregates, donor solvent coordination to the homometallic silyloxide building block can be undesirable for two reasons: (i) solvent blocks metal coordination sites which are necessary for elaboration of the homometallic into the polymetallic; (ii) if the solvent-derived coligands were carried along into the polymetallic aggregate, such coligands could provide sources of carbonaceous impurity during the ceramic conversion step. An additional advantage of our preparative method is that a bulky noncoordinating, volatile coproduct, hexamethyldisilazane, is formed, so the lanthanide silyloxide aggregate $[M(OSiPh_3)_3]_n$ can be isolated free of complications from amine coordination.

With respect to our goal of building polymetallic aggregates linked by –OR bridges, attention focused early on silyloxide complexes because of two anticipated desirable features. First, heterolytic Si–O bond cleavage leading to lanthanide-metal oxides should be disfavored because of the thermodynamic strength of the Si–O bond and the improbability of silyl cation formation. In contrast, heterolytic splitting of *carbon*–oxygen bonds in electropositive metal alkoxide complexes has been observed.[11,12] Indeed, initial efforts in this laboratory toward the preparation of tri-*tert*-butoxyyttrium derivatives invariably led to the obtention of a white, poorly soluble species, which could not be characterized further. 2-Propanol reacted with $[Y\{N(SiMe_3)_2\}_3]$ to yield the **oxo**–alkoxide aggregate $[Y_5(O^iPr)_{13}(O)]$.[23] Although oxo functionality is ultimately wanted, introduction of oxo groups at the homometallic stage could cause complications. Specifically, since oxo bridges in lanthanide-metal complexes are generally robust, homometallic lanthanide oxo–alkoxides may adopt aggregation states that are undesirably high and/or even unalterable. High aggregate nuclearity makes tailoring the metal stoichiometry in the final heteropolymetallic more difficult. Furthermore, O^{2-} is a potent donor and could diminish the Lewis acidity of the lanthanide(III) core, thereby making elaboration into polyheterometallic –OR bridged aggregates less favorable.

The other attractive feature of –$OSiR_3$ ligands concerns their weakly bridging nature. This should enable homometallic lanthanide aggregates to fragment to smaller units, thereby opening coordination sites at the metal. This is an important requirement for using $[M(OSiR_3)]_n$ reagents to construct $MM'(\mu\text{-}OSiR_3)$ linkages. Indeed, $[M(OSiPh_3)_3]_n$ aggregates reacted with a variety of neutral donors including THF, pyridine, and $(^nBu)_3PO$, to give **monomeric** species of general formula $[M(OSiPh_3)_3L_m]\cdot xL$ (M = Y, L = THF, m = 3, x = 1 (**3**); M = La, L = THF, m = 3, x = 1 (**4**); M = Y, L = pyridine, m = 3, x = 0 (**5**); M = La, L = pyridine, m = 3, x = 0 (**6**); M = Y, L = $(^nBu)_3PO$, m = 2,

(23) Coan, P. S. Unpublished observations.

$x = 0$, (**7**); M = La, L = $(^nBu)_3PO$, $m = 2$, $x = 0$, (**8**)). These results clearly demonstrate that **multiple** coordination sites are available at the lanthanide metal in **1** and **2**. In addition, the quantitative nature of many of these transformations is consistent with the formulation of **1** and **2** as homoleptic silyloxide complexes (i.e., devoid of oxide ligands).

The yttrium reagent, $[Y(OSiPh_3)_3]_n$, was elaborated into bimetallic silyloxide complexes by direct condensation with nucleophilic alkali-metal silyloxide reagents (eqs 1 and 2).[19] X-ray

$$[K(18\text{-crown-6})][OSiPh_3] + (1/n)[Y(OSiPh_3)_3]_n \rightarrow \underset{\mathbf{12}}{[K(18\text{-crown-6})][Y(OSiPh_3)_4]} \quad (1)$$

$$(1/m)[KOSiPh_3]_m + (1/n)[Y(OSiPh_3)_3]_n + DME \rightarrow \underset{\mathbf{11}}{[K(\eta^2\text{-DME})_3(\eta^1\text{-DME})][Y(OSiPh_3)_4(\eta^2\text{-DME})]} \quad (2)$$

analysis of one of these bimetallic derivatives, $[K(\eta^2\text{-DME})_3(\eta^1\text{-DME})][Y(OSiPh_3)_4(\eta^2\text{-DME})]$ (**11**) revealed the presence of *discrete*, well-separated K-centered cations and Y-centered anions. Formation of such separated ions may be undesirable from a molecular precursors perspective because the metal stoichiometry is no longer rigorously fixed on the molecular scale (i.e., in the reactive solution phase species). It may, however, be possible to discourage formation of separated ions by appropriate choices for ancillary ligands. In any case, complexes **11** and **12** may be valuable sources of $[Y(OSiPh_3)_4]^-$ nucleophiles, useful for constructing polymetallic aggregates via salt metathesis reactions employing metal halide coreactants. Such reactivity studies are in progress.

Another possible strategy for elaborating monometallic lanthanide silyloxide complexes into lanthanide-metal-containing polymetallic aggregates is outlined in Scheme I. Here the Bronsted acidity of a lanthanide *silyloxide–silanol* complex is exploited in a reaction with a reagent bearing a metal–ligand bond sensitive to protonolysis. Such a reaction could yield a heterometallic silyloxide aggregate, $[MM'(L)_m(OSiR_3)_4]$, along with the conjugate acid HG. In order to pursue this strategy, preparative routes to lanthanide silyloxide–silanol complexes were sought. We were *unable* to unambiguously characterize silyloxide–silanol complexes from reactions between triphenylsilanol and $[M(OSiPh_3)_3]_n$. However, the dinuclear yttrium complex $[\{Y(OSiMe_2{}^t\!Bu)_2(HOSiMe_2{}^t\!Bu)\}\{Y(OSiMe_2{}^t\!Bu)_2\}(\mu\text{-}OSiMe_2{}^t\!Bu)_2]$ (**9**) was synthesized in one step from $[Y\{N(SiMe_3)_2\}_3]$ and the tri*alkyl*silanol $HOSiMe_2{}^t\!Bu$. This compound features a five-coordinate Y center, bearing an $HOSiMe_2{}^t\!Bu$ ligand, linked to a four-coordinate Y center by two bridging $-OSiMe_2{}^t\!Bu$ groups. Complex **9** reacted with tetrahydrofuran to form *fac*-$[Y(OSiMe_2{}^t\!Bu)_3(THF)_3]$, demonstrating that (i) $HOSiMe_2{}^t\!Bu$ is only a weakly coordinating ligand and that (ii), consistent with our claims above, $-OSiMe_2{}^t\!Bu$ bridges to Y(III) cores are also weak. Efforts to exploit the Bronsted acidity of $[\{Y(OSiMe_2{}^t\!Bu)_2(HOSiMe_2{}^t\!Bu)\}\{Y(OSiMe_2{}^t\!Bu)_2\}(\mu\text{-}OSiMe_2{}^t\!Bu)_2]$ according to Scheme I by using metal amides as coreactants are currently underway.

Scheme I

$$[M(OSiR_3)_3(HOSiR_3)] + L_nM'\text{–}G \rightarrow [MM'(L)_m(OSiR_3)_4] + HG + (n-m)L$$

M = a lanthanide metal

M′ = any other metal

G = a uninegative ligand

L = ligand

Dynamic Solution Behavior: Mechanistic Conclusions. The six-coordinate Lewis base adducts $[M(OSiPh_3)_3(THF)_3]\cdot THF$ (M = Y (**3**), La (**4**)) and $[Y(OSiMe_2{}^t\!Bu)_3(THF)_3]$ (**10**) were found to be kinetically labile with respect to ligand exchange by ^1H NMR experiments. Thus, only a single set of THF-based resonances was detected when chloroform-d_1 solutions of the metal complexes were treated with free THF, indicating that ligand exchange was fast with respect to the NMR time scale (see supplementary material). Furthermore, as the relative concentration of tetrahydrofuran increased, the THF-based resonances asymptotically shifted toward those for free THF in $CDCl_3$. In an effort to probe the mechanism of the ligand exchange process, low-temperature ^1H NMR studies were conducted on a CD_2Cl_2 solution of **10**. At −90 °C, resonances of both **free** and coordinated THF were detected along with a second set of $-OSiMe_2{}^t\!Bu$-based signals. Such data are consistent with the freezing out of a dynamic equilibrium between **10** and a partially desolvated yttrium species (eq 3). A

$$[Y(OSiMe_2{}^t\!Bu)_3(THF)_3] \rightleftarrows (1/m)[Y(OSiMe_2{}^t\!Bu)_3(THF)_{3-n}]_m + nTHF \quad (3)$$

dissociative mechanism for THF exchange is thereby implicated. The solid-state composition and structures of $[M(OSiPh_3)_3(THF)_3]\cdot THF$ (M = Y, La) are consistent with this conclusion. Although the THF-to-metal ratio in these solids is 4:1, only **three** donors coordinate to the metal; the remaining THF simply fills a lattice void. Inspection of space-filling models for **3** and **4** reveals that a seven-coordinate complex would probably suffer severe nonbonded repulsions and is thus unattractive as a transition state for an associative mechanism for THF exchange.

The five-coordinate complex $[Y(OSiPh_3)_3\{(^nBu)_3PO\}_2]$ (**7**) was also found to be kinetically labile with respect to ligand exchange. Phosphorus-31 NMR monitoring of a toluene-d_8 solution of **7** containing 2 equiv of free $(^nBu)_3PO$ revealed two broad signals (58.0 and 48.5 ppm, respectively), which broadened further when the solution was warmed above room temperature. Line-shape analysis of these spectra gave an activation barrier for the exchange of 17 kcal/mol. However, the ^{31}P NMR signal for pure **7** in C_6D_6 is a sharp doublet (7.4 Hz), and the ^{89}Y NMR signal is a triplet with the same coupling constant. The observation of $^{31}P\text{–}^{89}Y$ coupling under these conditions is diagnostic of an **associative** mechanism for the phosphine oxide exchange process. Consistent with this conclusion, the rate of phosphine oxide exchange displays solvent dependence such that exchange is much slower in chloroform than in benzene or toluene. This effect is due to hydrogen bonding ($R_3PO\cdots H\text{–}CCl_3$)[24] which diminishes the nucleophilicity of the P=O moiety. Note that the rate of $(^nBu)_3PO$ exchange in CCl_4 is comparable to that in aromatic solvents, which rules out coordination of chlorocarbon as an alternative mechanistic explanation for these observations.

The complex $[K(\eta^2\text{-DME})_3(\eta^1\text{-DME})][Y(OSiPh_3)_4(\eta^2\text{-DME})]$ (**11**) is also fluxional in solution as shown by variable-temperature ^1H NMR spectroscopy (see supplementary material). At room temperature a single set of dimethoxyethane-based resonances were detected, indicating that exchange between Y-coordinated DME and K-coordinated DME is fast on the NMR time scale. This exchange is frozen out around −30 °C, and the DME region is then resolved into two sets of resonances. The DME-based resonances at and above 3.0 ppm were assigned to Y-coordinated groups. These chemical shifts are upfield of those for free dimethoxyethane and reflect the shielding influence of aromatic ring currents generated by the $-OSiPh_3$ substituents. A similar upfield shift in coordinated ligand resonances was detected in $[M(OSiPh_3)_3(THF)_3]\cdot THF$ (M = Y, La). No further changes in the DME region were apparent upon further cooling to −83 °C, which indicates that a DME arm-on/arm-off rearrangement at the seven-coordinate K^+ requires little activation energy.

In the phenyl region of the ^1H NMR spectrum of **11**, a simple pattern (ortho, doublet; meta, triplet; para triplet) was observed at room temperature indicating only one type of $-OSiPh_3$ group. This simple pattern persisted even at temperatures where DME exchange had been frozen out. When the solution was cooled further, resonances in the phenyl region broadened and finally resolved (−83 °C) into two sets in a 1:1 ratio, implying a solution structure consistent with the crystallographically determined structure featuring an octahedral Y(III) core with two $-OSiPh_3$ groups cis to the DME coligands and two $-OSiPh_3$ groups trans

(24) Maciel, G. E.; James, R. V. *Inorg. Chem.* **1964**, *3*, 1650.

Scheme II

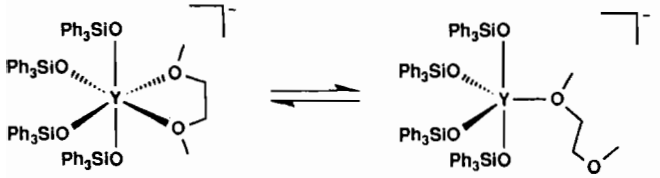

to the DME coligands. A mechanism for this fluxional behavior is postulated in Scheme II. Dissociation of one DME oxygen from the **six**-coordinate yttrium center represents a mechanism analogous to that observed for the six-coordinate THF adduct **10**. Furthermore, the resulting five-coordinate complex is expected to be stereochemically nonrigid, easily equilibrating $-OSiPh_3$ groups via pseudorotation.

The complex $[\{Y(OSiMe_2{}^tBu)_2(HOSiMe_2{}^tBu)\}\{Y(OSiMe_2{}^tBu)\}(\mu\text{-}OSiMe_2{}^tBu)_2]$ (**9**) was also observed to be fluxional in solution. In CD_2Cl_2 only a single set of $-OSiMe_2{}^tBu$-based resonances was detected along with a broad singlet resonance for the hydroxyl hydrogen down to −80 °C. This experiment demonstrated a very low activation energy requirement for stereochemical rearrangements, presumably reflecting inter alia the facility with which the acidic hydroxyl proton can exchange among the various oxygen sites.

In summary, ligand reorganizations in yttrium(III) and lanthanide(III) silyloxides are common, low-energy processes. This fact has an important practical implication; namely, it is often difficult to deduce complex structure by using solution-based spectroscopic methods, typically NMR. Consequently, product identification must rely heavily on single-crystal X-ray diffraction analysis. The corollary that solid-state structures may (and we believe often do) differ significantly from solution-phase structures in yttrium(III) and lanthanide silyloxides is self-evident.

Structural Comparisons and Bonding Considerations. Of the lanthanide metal(III) ions, lanthanum(III) has the largest radius while yttrium(III) (although not a true lanthanide) has one of the smallest.[25] Differences in the chemistry of a given metal(III) complex across the lanthanide series tend to reflect variations in ion size. Complexes $[Y(OSiPh_3)_3(THF)_3]\cdot THF$ (**3**) and $[La(OSiPh_3)_3(THF)_3]\cdot THF$ (**4**) were prepared by analogous procedures, displayed similar reactivity patterns (ligand exchange), and were found to be crystallographically *isomorphous*. These observations imply that for a given $-OSiR_3$ ligand set, the chemistry and structural properties of the derived metal(III) complexes across the series are expected to be very similar.

For the three yttrium (triphenylsilyl)oxide complexes $[Y(OSiPh_3)_3(THF)_3]\cdot THF$ (**3**), $[Y(OSiPh_3)_3\{(n\text{-}Bu)_3PO\}_2]$ (**7**), and $[K(\eta^2\text{-DME})(\eta^2\text{-DME})][Y(OSiPh_3)_4(\eta^2\text{-DME})]$ (**11**), a trend in the Y–OSi distances can be discerned: **7** (five-coordinate Y) ≤ **3** (six-coordinate Y) < **11** (six-coordinate Y, anionic). A similar trend is evident for the (alkylsilyl)oxide derivative $[\{Y(OSiMe_2{}^tBu)_2(HOSiMe_2{}^tBu)\}\{Y(OSiMe_2{}^tBu)_2\}(\mu\text{-}OSiMe_2{}^tBu)_2]$ (**9**), where Y(1) (five-coordinate) has longer Y–OSi bond distances (for both bridging and terminal groups) than Y(2) (four-coordinate). These trends are consistent with a bonding model for lanthanide silyloxide complexes in which electrostatic attraction makes an important contribution. Consistent with this claim, a comparison of terminal Y–OSi distances for five-coordinate Y(III) cores (**7** and Y(1) of **9**) reveals that $-OSiMe_2{}^tBu$ binds more tightly than $-OSiPh_3$. This difference can be rationalized by taking into account the greater electron-releasing ability of alkyl groups vs aryl groups, which presumably makes $-OSiMe_2{}^tBu$ more nucleophilic at oxygen than $-OSiPh_3$.

Lanthanide-metal dπ–oxygen pπ interactions also contribute to the bonding in these silyloxide complexes. The clearest evidence for this stems from the exclusively facial orientation found for both **3** and **4**. The facial conformation maximizes O(pπ)→M(dπ) bonding because competition for the set of three vacant dπ functions at the metal is minimized. The energy gain from such bonding is apparently sufficient to overcome the increased interligand repulsions expected for the facial conformer vis-á-vis the meridonal one. The large values measured for the M–O–Si angles (158–180°) also indicate oxygen–metal multiple bonding. However, our data show that this structural parameter is not sensitively correlated with M–OSi distances. For example in $[Y(OSiPh_3)_3\{(^nBu)_3PO\}_2]$ the Y–OSi distances vary by only 0.01 Å while the Y–O–Si angles vary by nearly 20°. The M–O–Si angles are apparently quite malleable, doubtless strongly influenced by steric pressures.[26]

Table X also cites silyloxide Si–O bond distances. The largest Si–O separations are associated with the shortest Y–O separations (e.g., in **9**), but a consistent pattern in these data is not apparent.

Conclusions

Homoleptic yttrium and lanthanum silyloxide complexes, $[M(OSiPh_3)_3]_n$, are available by reaction of triphenylsilanol with $[M\{N(SiMe_3)_2\}_3]$. Reaction of the metal amide with 3.5 equiv of the trialkylsilanol $HOSiMe_2{}^tBu$ gave the silyloxide–silanol complex $[\{Y(OSiMe_2{}^tBu)_2(HOSiMe_2{}^tBu)\}\{Y(OSiMe_2{}^tBu)_2\}(\mu\text{-}OSiMe_2{}^tBu)_2]$. Reactivity studies showed that silyloxide bridges in lanthanide complexes are weak, efficiently opening to make multiple coordination sites available at the metal(III) core.

Many of the Lewis base adducts reported here were found to be kinetically labile with respect to ligand exchange. NMR studies supported the contention that six-coordinate complexes participate in ligand exchange via a dissociative mechanism, whereas the five-coordinate complex $[Y(OSiPh_3)_3\{(^nBu)_3PO\}_2]$ undergoes ligand exchange via an associative pathway.

X-ray diffraction studies on several of the compounds reported here indicated a bonding model wherein electrostatic attraction contributed significantly. Notwithstanding, large M-O-Si angles and the facial orientation of the -$OSiPh_3$ groups in $[Y(OSiPh_3)_3(THF)_3]\cdot THF$ and $[La(OSiPh_3)_3(THF)_3]\cdot THF$ revealed that silyloxide oxygen pπ(filled)→metal dπ(vacant) interactions are also important to the bonding description of lanthanide silyloxide complexes.

Acknowledgment. This work was supported by the Department of Energy. We thank Scott Horn for skilled technical assistance.

Supplementary Material Available: Figures showing NMR spectra of **3** and **11** and tables listing full crystallographic details and anisotropic thermal parameters for **3**, **4**, **7**, **9**, and **11** (13 pages); tables of observed and calculated structure factors for **3**, **4**, **7**, **9**, and **11** (65 pages). Ordering information is given on any current masthead page.

(25) Shannon, R. D. *Acta. Crystllogr.* **1976**, *A32*, 751.

(26) For an alternative view, see: Shambayati, S.; Blake, J. F.; Wierschke, S. G.; Jorgensen, W. L.; Schreiber, S. L. *J. Am. Chem. Soc.* **1990**, *112*, 697.